

Assessment of the MACC reanalysis and its influence as chemical boundary conditions for regional air quality modeling in AQMEII-2

L. Giordano^a, D. Brunner^{a,*}, J. Flemming^b, C. Hogrefe^c, U. Im^{d,1}, R. Bianconi^e, A. Badia^f, A. Balzarini^g, R. Baró^h, C. Chemelⁱ, G. Curci^j, R. Forkel^k, P. Jiménez-Guerrero^h, M. Hirtl^l, A. Hodzic^m, L. Honzakⁿ, O. Jorba^f, C. Knote^m, J.J.P. Kuenen^o, P.A. Makar^p, A. Manders-Groot^o, L. Neal^q, J.L. Pérez^r, G. Pirovano^g, G. Pouliot^s, R. San José^r, N. Savage^q, W. Schröder^t, R.S. Sokhiⁱ, D. Syrakov^u, A. Torian^c, P. Tuccella^j, J. Werhahn^k, R. Wolke^t, K. Yahya^v, R. Žabkar^{n,w}, Y. Zhang^v, S. Galmarini^d

^a Laboratory for Air Pollution and Environmental Technology, EMPA, Duebendorf, Switzerland

^b ECMWF, Shinfield Park, RG2 9AX Reading, United Kingdom

^c Atmospheric Modelling and Analysis Division, Environmental Protection Agency, Research Triangle Park, USA

^d Institute for Environment and Sustainability, Joint Research Centre, European Commission, Ispra, Italy

^e Enviroware Srl, Concorezzo, MB, Italy

^f Earth Sciences Department, Barcelona Supercomputing Center (BSC-CNS), Barcelona, Spain

^g RSE S.p.A., Milano, Italy

^h University of Murcia, Department of Physics, Physics of the Earth, Campus de Espinardo, Ed. CIOyN, 30100 Murcia, Spain

ⁱ Centre for Atmospheric & Instrumentation Research, University of Hertfordshire, College Lane, Hatfield AL10 9AB, UK

^j Department of Physical and Chemical Sciences, Center of Excellence for the forecast of Severe Weather (CETEMPS), University of L'Aquila, L'Aquila, Italy

^k Karlsruhe Institut für Technologie (KIT), IMK-IFU, Kreuzteckbahnstr. 19, 82467 Garmisch-Partenkirchen, Germany

^l Section Environmental Meteorology, Division Customer Service, ZAMG – Zentralanstalt fuer Meteorologie und Geodynamik, 1190 Wien, Austria

^m National Center for Atmospheric Research, Boulder, CO, USA

ⁿ Center of Excellence SPACE-SI, Ljubljana, Slovenia

^o Netherlands Organization for Applied Scientific Research (TNO), Utrecht, The Netherlands

^p Air Quality Research Section, Atmospheric Science and Technology Directorate, Environment Canada, 4905 Dufferin Street, Toronto, Ontario, Canada

^q Met Office, FitzRoy Road, Exeter EX1 3PB, United Kingdom

^r Environmental Software and Modelling Group, Computer Science School – Technical University of Madrid, Campus de Montegancedo – Boadilla del Monte, 28660 Madrid, Spain

^s Atmospheric Modeling and Analysis Division, MD E243-04, U.S. Environmental Protection Agency, Research Triangle Park, NC 27711, USA

^t Leibniz Institute for Tropospheric Research, Permoserstr. 15, D-04318 Leipzig, Germany

^u National Institute of Meteorology and Hydrology, Bulgarian Academy of Sciences, Sofia, Bulgaria

^v Department of Marine, Earth and Atmospheric Sciences, 2800 Faucette Drive, Jordan Hall, Campus Box 8208, North Carolina State University, USA

^w University of Ljubljana, Faculty of Mathematics and Physics, Ljubljana, Slovenia

ARTICLE INFO

Article history:

Received 9 June 2014

Received in revised form

20 January 2015

Accepted 10 February 2015

Available online 12 February 2015

Keywords:

Online-coupled meteorology-chemistry

modeling

Model evaluation

AQMEII-2

ABSTRACT

The Air Quality Model Evaluation International Initiative (AQMEII) has now reached its second phase which is dedicated to the evaluation of online coupled chemistry-meteorology models. Sixteen modeling groups from Europe and five from North America have run regional air quality models to simulate the year 2010 over one European and one North American domain. The MACC re-analysis has been used as chemical initial (IC) and boundary conditions (BC) by all participating regional models in AQMEII-2. The aim of the present work is to evaluate the MACC re-analysis along with the participating regional models against a set of ground-based measurements (O_3 , CO, NO, NO_2 , SO_2 , SO_4^{2-}) and vertical profiles (O_3 and CO). Results indicate different degrees of agreement between the measurements and the MACC re-analysis, with an overall better performance over the North American domain. The influence of BC on regional air quality simulations is analyzed in a qualitative way by contrasting model performance for the MACC re-analysis with that for the regional models. This approach complements more quantitative

* Corresponding author.

E-mail address: dominik.brunner@empa.ch (D. Brunner).

¹ Now at: Aarhus University, Department of Environmental Science, Frederiksborgvej 399, 4000, Roskilde, Denmark.

approaches documented in the literature that often have involved sensitivity simulations but typically were limited to only one or only a few regional scale models. Results suggest an important influence of the BC on ozone for which the underestimation in winter in the MACC re-analysis is mimicked by the regional models. For CO, it is found that background concentrations near the domain boundaries are rather close to observations while those over the interior of the two continents are underpredicted by both MACC and the regional models over Europe but only by MACC over North America. This indicates that emission differences between the MACC re-analysis and the regional models can have a profound impact on model performance and points to the need for harmonization of inputs in future linked global/regional modeling studies.

© 2015 The Authors. Published by Elsevier Ltd. This is an open access article under the CC BY-NC-ND license (<http://creativecommons.org/licenses/by-nc-nd/4.0/>).

1. Introduction

Modeling plays an important role in the integrated assessment of air quality issues, contributing to strengthening the understanding and characterization of air pollution and eventually leading to well-informed air quality management decisions and strategies. Regional air quality modeling has been the focus of considerable development during recent decades, driven by increased concern regarding the impact of air pollution on human health and the ecosystem. Numerous air quality models have been developed by research groups worldwide and are being widely used for designing emission control policies and forecasting air quality. However, unlike other geophysical sciences such as climatology, there have only been limited coordinated international efforts to study and evaluate the performance of the air quality models.

Since 2008, the Air Quality Model Evaluation International Initiative (AQMEII, Rao et al., 2010) coordinated by the European Joint Research Center (JRC), the U.S. Environmental Protection Agency (EPA), and Environment Canada (EC), has promoted research on regional air quality model evaluation across the atmospheric modeling communities of Europe and North America. AQMEII has now reached its second phase which is dedicated to the evaluation of online coupled chemistry-meteorology models, as opposed to Phase 1 where only offline models were considered. At the European level, AQMEII collaborates with the COST Action European framework for online integrated air quality and meteorology modeling (EuMetChem, <http://eumetchem.info>). AQMEII-2 has the goal of validating the many different models used to estimate air quality at local levels around the world, how these models might be used in ensemble simulations and whether these models can be used to simulate feedbacks between weather and chemistry and to predict ways in which climate change will interact with air quality.

Two spatial domains were used in the exercise - one over Europe and one over North America. All groups participating in AQMEII-2 performed simulations on one or both of these domains using the same input data. Simulation outputs were regridded onto the same horizontal and vertical grid and, for comparison with observations, were interpolated to prescribed sets of measurement station locations (receptors). All outputs were collected, together with evaluation data sets (including measurements from surface in-situ networks from AirBase and EMEP, vertical profiles from ozonesondes and aircraft from MOZAIC, and ground-based remote sensing from AERONET), by the JRC.

Regional models need to constrain the concentrations at the domain boundaries: the initial and lateral boundary conditions (IC, BC hereafter) were shared between all groups and were provided by the MACC re-analysis of the IFS-MOZART model ("MACC re-analysis" hereafter) (Stein et al., 2011; Inness et al., 2013). Emissions were provided by the TNO/MACC database for anthropogenic emissions for the European domain and by U.S. EPA for the North

American domain.

The focus of the present paper is on performing an operational evaluation (Dennis et al., 2010) of the MACC re-analysis data in the same way as all the regional models participating in AQMEII-2 have been evaluated (Im et al., 2015a,b; Brunner et al., 2015) and to assess its influence as chemical BC. The current study complements the work by Im et al. (2015a,b) by expanding the list of variables that are analyzed and by systematically contrasting seasonal and spatial patterns of model performance for the MACC re-analysis with the performance of the regional models. It also complements the work of Inness et al. (2013) by evaluating the MACC re-analysis fields for additional pollutants (NO, SO₂, sulfate) and at additional monitoring sites. It should be noted that for a full quantification of the influence of BC on the results of regional models, sensitivity simulations with varying BC would need to be performed by the regional models. Such sensitivity simulations were beyond the scope of the second Phase of AQMEII. A limited quantitative analysis was performed by Hogrefe et al. (2014) for ozone over the North American domain for the months January and July. Replacing the MACC re-analysis by the GEMS re-analysis used during AQMEII phase 1 had a significant impact on near-surface ozone concentrations with differences of the order of 7 ppb over large portions of the domain in January and 3 ppb in July.

Here, we analyze the influence of BC in a more qualitative way by evaluating the performance of the MACC re-analysis and by analyzing the differences between its results and those of the participating models. This phenomenological analysis of one global model in comparison to a large number of regional models driven by boundary conditions from this global model complements more quantitative approaches documented in the literature that often have involved sensitivity simulations but typically were limited to only one or only a few regional scale models (e.g. Makar et al., 2010; Katragkou et al., 2010; Hogrefe et al., 2011; Schere et al., 2012). In addition, none of these earlier studies investigated the impact of boundary conditions on regional air quality model performance over two continents in a systematic manner.

In air quality numerical simulations, the influence of the BC on the results in the interior of the model domain varies strongly from species to species depending on its lifetime. For species with a lifetime comparable or exceeding the average time it takes to transport an air mass across the model domain, the BC will potentially have a large influence on the modeling results. Therefore, we evaluate the MACC re-analysis against observations for a range of species provided as BC for the regional models with a large range of different lifetimes, and compare the results of the MACC re-analysis with the results of the regional models. For longer lived species we expect the regional models to follow more closely the MACC re-analysis, whereas for shorter lived species the differences may be larger and dominated by differences in emissions within the model domain or differences in photochemistry, deposition, and other factors. In cases where concentrations of longer-lived

species with large primary sources such as CO differ between the MACC re-analysis and the regional-scale models, these differences may point to inconsistencies in the emission inventories used in the global and regional scale simulations. Documenting such instances in this study will provide motivation for future work aimed at better linking global and regional scale modeling systems, including a harmonization of emission inventories.

Since this study compares domain-averaged results from the regional models with both the MACC re-analysis and with observations, it also presents a limited evaluation of the regional models for a range of species for which the MACC reanalysis provided the boundary conditions (O_3 , CO, NO_x , SO_2 , SO_4^{2-}). While O_3 and $PM_{2.5}$ concentrations from the regional models have already been analyzed by Im et al. (2015a,b), the current study complements this work by including additional species and explicitly contrasting model performance between the global and regional models.

2. Models

2.1. Regional models participating in AQMEII phase 2

In the context of AQMEII-2, 16 models from Europe (EU) and 5 models from North America (NA) have been used to simulate the year 2010 (see Table 1). Only one model (BG2) has been run offline, while the other models are online coupled. The online coupled models are separated into online access models (NL2, UK5, DE3 and US6) and online integrated models (all the remaining). Online access models are defined as models that use independent meteorology and chemistry modules that might even have different grids, but exchange meteorology and chemistry data on a regular and frequent basis. In contrast, online integrated models simulate meteorology and chemistry over the same grid in one model using one main time step for integration as defined in (Baklanov et al., 2014).

Nine groups used the WRF-Chem model (Grell et al., 2005) and its variant (e.g., Wang et al., 2015), having different gas-phase mechanisms but similar aerosol modules that employ different size distributions approaches (modal/bin and inorganic/organic aerosol treatments). The IT2 simulation is performed with an experimental version of WRF-Chem v. 3.4, where the new secondary organic aerosol scheme VBS is coupled to the aerosol indirect effects modules.

Table 1
Overview of participating models.

Domain	Group	Specifications	Model
EU	BG2	offline	WRF-CMAQ
EU	NL2	access online	RACMO LOTUS-EUROS
EU	DE3	access online	COSMO-MUSCAT
EU	UK5	access online	WRF-CMAQ
NA	US6	access online	WRF-CMAQ
EU	AT1	integrated online	WRF-CHEM
EU	DE4	integrated online	WRF-CHEM
EU	ES1	integrated online	WRF-CHEM
EU	ES3	integrated online	WRF-CHEM
EU	IT1	integrated online	WRF-CHEM
EU	IT2	integrated online	WRF-CHEM
EU	SI1	integrated online	WRF-CHEM
EU	US6	integrated online	WRF-CHEM
EU	US8	integrated online	WRF-CHEM
EU	CH1	integrated online	COSMO-ART
EU	ES2a	integrated online	NMMB-BSC-CTM
EU	ES2b	integrated online	NMMB-BSC-CTM
EU	UK4	integrated online	METUM-UKCA RAQ
NA	CA2	integrated online	GEM-MACH
NA	CA2f	integrated online	GEM-MACH

Anthropogenic emissions for AQMEII-2 were provided by U.S. EPA for North America (Pouliot et al., 2015), and TNO (Nederlandse Organisatie voor Toegepast Natuurwetenschappelijk Onderzoek) for Europe (Kuenen et al., 2014, Pouliot et al., 2015). Each participating group had the freedom to choose a grid coordinate system that should however cover the prescribed domains (EU or NA). Emissions were therefore re-gridded for each model. Pouliot et al. (2015) provides quantitative explanations of the aerosol loading in the coupled model runs for 2010 and a quantitative analysis of changes in emissions between 2006 and 2010. Biomass burning emissions for the European domain were provided by FMI (<http://is4fires.fmi.fi/>) and by SMART-FIREv2 for NA. Other natural emissions such as sea salt, mineral dust or biogenic VOCs were not prescribed but simulated online by the individual models.

The simulations were conducted for continental-scale domains of EU and NA covering the continental U.S., southern Canada and northern Mexico. To facilitate the cross-comparison between models, the participating groups interpolated their model output to a common regular grid with 0.25° resolution for both continents. The native grids used by the different groups varied in both resolution and grid projection but typically had a resolution on the order of 0.25° (Im et al., 2015a; Brunner et al., 2015). In addition, model values at observation stations (receptors) were obtained by interpolation from the original model output files for comparison to observations.

2.2. Global IFS-MOZART model providing chemical boundary conditions

The chemical BC for all models were provided by ECMWF from the MACC re-analysis (Inness et al., 2013). The MACC re-analysis uses an updated data set of anthropogenic emissions (MACCity, (Granier et al., 2011)) with assimilation of satellite observations of O_3 , CO and NO_2 in the coupled system IFS-MOZART (Flemming et al., 2009). It produced a 10 year long reanalysis of global atmospheric composition for the period 2003–2012. As pointed out in Inness et al. (2013), the assimilation of satellite observations of O_3 , CO, and NO_2 greatly improved total column values, that are generally in very good agreement with independent observations, but profiles can show some problems in the boundary layer where concentrations are dominated by emissions. Moreover, most of the assimilated satellite observations had little sensitivity to pollutants near the surface and very coarse (or no) vertical resolution in the troposphere and therefore provided fewer constraints on concentrations in the planetary boundary layer.

MACC data are available in 3-h time intervals and were provided in daily files with 8 times per file. The horizontal resolution of the model is $1.125^\circ \times 1.125^\circ$. Variables were provided as 3D fields in pressure hybrid vertical coordinates and included gas phase species (O_3 , NO, NO_2 , HNO_3 , HO_2 , NO_2 , OH, H_2O_2 , CO, CH_4 , PAN, SO_2 , CH_2O (formaldehyde), C_2H_6 (ethane), CH_3CHO (acetaldehyde), BIGENE (C > 3 alkenes and alkynes), BIGALK (C > 3 alkanes), ISOP (isoprene), TOLUENE) and aerosol species (sea-salt, dust, sulfate, organic matter and black carbon. Note: Organic matter and black carbon were described as sum of hydrophobic and hydrophilic). NMVOC species had to be assigned to the most closely matching chemical species depending on the individual model's chemical speciation.

In order to mitigate known biases and issues in the MACC data, a list of recommendations were formulated for the modelers to follow. The organic aerosol concentrations were assigned to primary organic aerosol (POA) since it is unclear how this should be distributed on secondary organic aerosol (SOA) in a given model. Since a preliminary analysis indicated that MACC sea-salt fields were significantly biased high, they were not used as input to the

regional models, but the simulation grids were large enough such that each model could generate the sea salt fields internally using its own sea salt parameterization. Mineral dust aerosols were provided by MACC in three different size ranges (0.03–0.55 μm , 0.55–0.9 μm and 0.9–20 μm) which had to be mapped onto the aerosol size classes used by each of the regional models. The guideline was to use a simple but mass-conserving mapping while taking into account the fact that the IFS-MOZART model used in MACC placed a too large fraction of total dust mass into the smallest size bin, a deficiency that was improved in 2012 for the near-real-time analysis product (Jean-Jacques Morcrette, ECMWF, personal communication). It was therefore advised to shift the MACC total dust aerosol mass from the size bins listed above to larger size ranges in the regional models whenever possible, e.g. by summing up the masses of the three size ranges and then attributing 10% to fine and 90% to coarse mineral dust, following Johnson and Osborne (2011).

3. Observations and evaluation method

3.1. Surface observations

The 2010 hourly measurements of surface concentrations of O_3 , CO, SO_2 , NO, NO_2 and SO_4^{2-} aerosol were provided by EMEP (European Monitoring and Evaluation Programme, <http://www.emep.int/>) and AirBase (<http://acm.eionet.europa.eu/databases/airbase/>) in Europe. In North America they were provided by AIRS (Aerometric Information Retrieval Systems, <http://www.epa.gov/air/data/aqsdb.html/>) and NAPS (National Air Pollution Surveillance, <http://www.ec.gc.ca/rnspa-naps/>). The data were homogenized and ingested into the ENSEMBLE system (Galmarini et al., 2012) by the JRC for the EU case, and by Environment Canada for the NA case. Weekly/bi-weekly CO measurements from the NOAA/GMD flask sampling network (Novelli and Masarie, 2009) were obtained from WDCGG (World Data Centre for Greenhouse Gases, <http://ds.data.jma.go.jp/gmd/wdogg/>) and were not used in any other AQMEII Phase 2 studies such as Im et al. (2015a,b).

3.2. Vertical profiles

The 2010 vertical profiles at selected airports were provided by MOZAIC (<http://www.iagos.fr/web/rubrique2.html>). The MOZAIC program is designed to collect O_3 , CO and water vapor data using automatic equipment installed on-board several long-range passenger airliners flying regularly from Europe to destinations all over the world. Five long-range passenger aircrafts carry MOZAIC instruments and visit 35 different airports around the world. Measurements of O_3 are taken every four seconds from takeoff to landing and have an accuracy of $\pm(2 \text{ ppbv} + 2\%)$ (Thouret et al., 1998). Measurements of CO are taken every 30 s from takeoff to landing and have an accuracy of $\pm(5 \text{ ppbv} \pm 5\%)$ (Nédélec et al., 2003). The original MOZAIC data set is separated into cruising (for which data are temporally averaged) and landing/take off phase (for which data are averaged over 100 m vertical intervals). The MOZAIC data considered here were gathered during takeoff and landing phases at the airport of Frankfurt, with the majority of data being in the morning hours between 07 and 12 UTC. Unfortunately, data coverage in 2010 was much poorer than in other years and was limited to the winter and fall seasons (Solazzo et al., 2013). For this analysis we use measurements at Frankfurt airport location, ingested into the ENSEMBLE system by the JRC to provide measurements at a set of 13 fixed elevations above ground.

3.3. Evaluation method

Each modeling group has provided standardized outputs: hourly maps of surface concentrations, re-gridded to the same horizontal resolution of $0.25^\circ \times 0.25^\circ$, hourly surface concentrations at selected locations (receptor points) and vertical profiles at airport locations. The same standardized output has been extracted from MACC, i.e. MACC fields were interpolated to the common $0.25^\circ \times 0.25^\circ$ analysis grid for the analysis of gridded fields and to the location of the selected monitoring sites for the analysis at specific receptor locations.

For the present analysis, we retrieved CO, O_3 , NO, NO_2 , SO_2 and SO_4^{2-} aerosol receptor data from the ENSEMBLE system to compare against station observations. This selection is motivated by the requirement that the species should be provided as BC by the MACC re-analysis, that there should be a sufficient number of observations available for validation, and that the compounds should cover a range of lifetimes. Since the regional models use relatively coarse horizontal resolutions (see also Table 1 in Im et al. (2015a)), we compare surface concentrations only at rural sites, selecting stations with data availability greater than 75% and altitudes lower than 1000 m ASL. The number of stations with available measurements according to this selection is shown in Table 2. We mainly focus on midday/afternoon values (12–14 UTC over EU, 19–21 UTC over NA) because models are known to have difficulties in representing the nighttime boundary layer accurately (Steenefeld et al., 2006; Brunner et al., 2015). The model outputs were first time-averaged for each month and then averaged over all selected stations.

For surface concentration maps, we have computed seasonal multi-model means. EU data were converted to ppb using the provided standard pressure and temperature to be directly comparable with NA data.

Model performance is quantified through mean, normalized mean bias (NMB), root mean square error (RMSE) and Pearson's correlation coefficient.

4. Results

4.1. Evaluations of the models against surface observations

4.1.1. O_3

O_3 is one of the most important photooxidants in the atmosphere. High surface O_3 concentrations are of concern as they can cause serious problems to human health and vegetation. It is not emitted directly into the air, but in the troposphere it is formed via photochemical cycles involving volatile organic compounds (VOC) and oxides of nitrogen (NO_x). These precursors of ozone have both natural and anthropogenic sources both of which are accounted for in the models analyzed in this study.

O_3 results were extensively discussed in Im et al. (2015a), where it was found that the MACC re-analysis has a large diurnal amplitude, with too high values during day and too low values during

Table 2
Stations selection.

Chemical species	Number of stations	
	EU	NA
O_3	401	271
CO	48	17
NO	211	15
NO_2	285	59
SO_2	165	44
SO_4	33	70

night. We extended their analysis by looking separately at the median monthly midday values (Fig. 1) and midnight values (Fig. 2). In Table 3 we report performance metrics for all the models, focusing on winter and summer midday periods. The MACC re-analysis midday median values over EU show a strong seasonal cycle, with an underestimation in the winter season (NMB = -26.0%) and an overestimation in summer (NMB = 26.4%). On the other hand, MACC re-analysis midnight values consistently underestimate O_3 throughout the year. This overestimation of the amplitude of the diurnal cycle of O_3 was also reported by Inness et al. (2013) but the reasons could not be identified. This problem is reduced in the new fully integrated model C-IFS (Flemming et al., 2014). Neither MACC nor the regional models capture the elevated observed concentrations during springtime, a shortcoming that has also been pointed out by Inness et al. (2013) for the MACC fields. The underestimation of ozone in the regional models during these months is thus likely driven by too little ozone entering the domain through the lateral boundaries. Over NA, the MACC re-analysis median values are closer to the observations, both during daytime and nighttime, only overestimating midday O_3 in the month of July.

4.1.2. CO

CO affects the concentrations of O_3 and the OH radical, and therefore plays a fundamental role in global tropospheric chemistry. Anthropogenic sources account for roughly two thirds of all CO emissions (Seinfeld and Pandis, 2006) through combustion of biomass and fossil fuel; in fact, the highest concentrations of CO are found in highly industrialized regions. Wildfires are another important source, originating mostly from tropical forest fires but receiving contributions as high as 25% from boreal forest fires in some years (Goode et al., 2000). Photochemical oxidation of methane and non-methane hydrocarbons is another important source which is estimated to represent more than half of the total source of CO globally, larger than direct emission (Duncan et al.,

2007).

CO is the longest lived species that has been simulated by all models, including MACC re-analysis, and for which we have available observations.

The MACC re-analysis for reactive gases has been extensively evaluated in Inness et al. (2013) and Stein et al. (2014). In particular, surface CO was found to agree well with NOAA/GMD observations at a selection of remote sites (Mace Head, Key Biscayne, Tenerife and South Pole); total column values were in good agreement with observations, but vertical profiles showed some differences from observations in the boundary layer (Inness et al., 2013). Since boundary layer concentrations are dominated by emissions, these differences could be an indication of errors in the emission inventory for CO (and VOCs), underestimation of the chemical source, a lack of efficacy in modeling boundary layer mixing processes, and/or a mismatch in the spatial representativeness of the observations and MACC fields, but no further diagnostic analysis of the relative importance of these potential factors was presented in Inness et al. (2013).

In order to conduct a more comprehensive comparison within the AQMEII-2 modeling domains, we have selected a sample of four NOAA/GMD flask sampling sites (Novelli and Masarie, 2013), two for each domain, of which one is representative of remote conditions, as close as possible to the domain border (Mace Head for EU and Key Biscayne for NA), and one station is located in the middle of the domain (Black Sea EU and Park Falls for NA). Fig. 3 shows CO concentrations from the MACC model compared with measurements at these selected stations. At the remote stations near the domain boundaries (Mace Head and Key Biscayne) the model agrees well with the observations, while there are differences between observations and MACC fields at the Park Falls and Black Sea sites. In particular, the MACC re-analysis exhibits a moderate level of underprediction at the Park Falls site for most of spring and summer, while there is a large negative bias, particularly in winter, at the Black sea site similar to the biases observed at other sites over

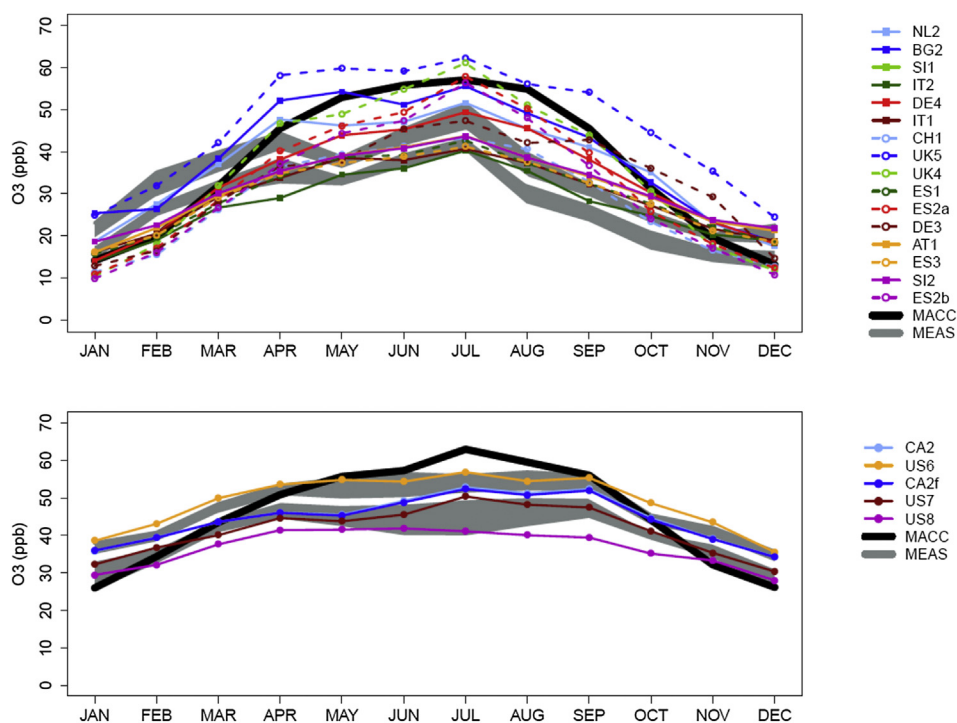


Fig. 1. Time series for 2010 of median monthly O_3 concentrations, midday values, for EU (top, 12–14 UTC) and NA (bottom, 19–21 UTC) domains. The gray shaded area is the interquartile range of the distribution of observations across all selected stations. The white line represents the median of the observations.

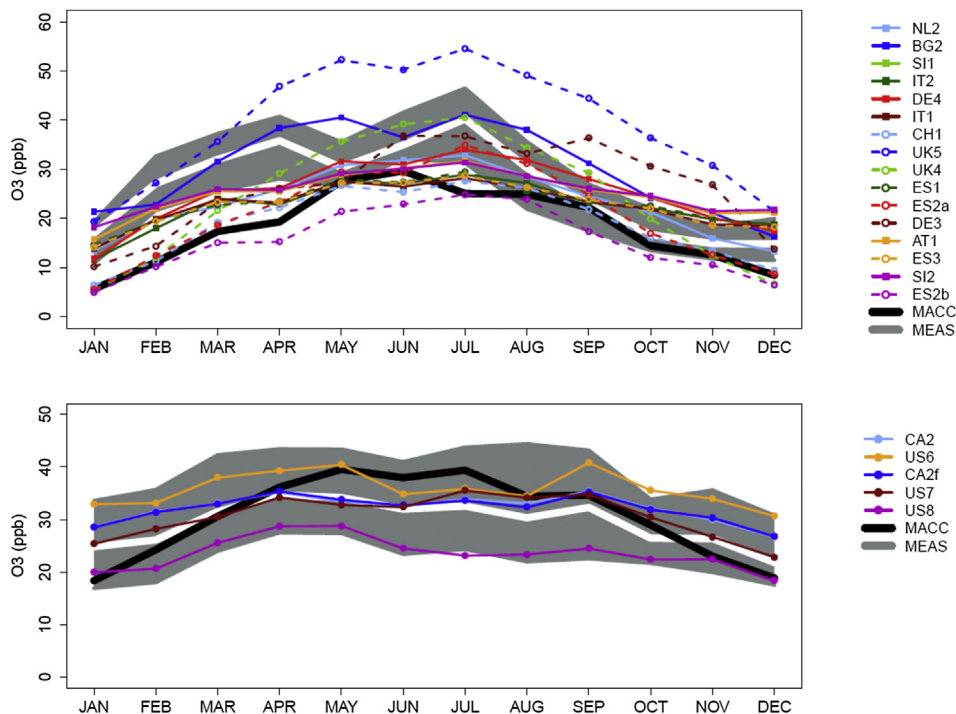


Fig. 2. Time series for 2010 of median monthly O₃ concentrations, midnight values, for EU (top, 00–02 UTC) and NA (bottom, 07–09 UTC) domains. The gray shaded area is the interquartile range of the distribution of observations across all selected stations. The white line represents the median of the observations.

continental Europe (see below). As explained in Inness et al. (2013) and Stein et al. (2014), the emission inventory (MACCity) used by the re-analysis might be the primary source of such large negative biases.

In Fig. 4 we show the midday median monthly CO surface concentrations for 48 European and 17 North American rural stations with continuous measurements. In Table 4 we report

Table 3 Seasonal (summer and winter) midday model performance metrics for O₃ at ground stations.

Model	O ₃							
	Mean (ppb)		NMB (%)		RMSE (ppb)		r	
	S	W	S	W	S	W	S	W
MACC (EU)	54.01	18.37	26.4	-26.04	16.43	11.94	0.58	0.51
BG2	50.47	27.23	17.98	9.68	14.65	15.97	0.56	0.31
NL2	46.78	22.55	9.4	-9.23	12.14	10.1	0.64	0.5
DE3	44.33	17.52	3.65	-29.41	12.31	13.07	0.54	0.41
UK5	56.76	29.44	32.8	18.64	18.29	11.07	0.62	0.53
AT1	41.12	21.43	-3.81	-13.67	11.22	10.92	0.63	0.42
DE4	46.05	19.79	7.7	-20.32	11.8	11.43	0.62	0.47
ES1	39.35	20.11	-7.96	-19.01	11.64	11.31	0.63	0.41
ES3	38.64	20.5	-9.61	-17.41	12.14	10.8	0.61	0.49
IT1	37.92	20.57	-11.3	-17.18	12.62	10.83	0.58	0.49
IT2	35.27	19.69	-17.53	-20.59	13.47	11.34	0.63	0.48
SI1	41.2	22.48	-3.62	-9.47	11.29	10.39	0.63	0.43
SI2	41.07	22.54	-3.94	-9.21	11.26	10.32	0.63	0.44
CH1	41.52	15.78	-2.9	-36.46	13.84	13.23	0.48	0.53
ES2a	50.36	16.61	17.8	-33.12	14.75	13.22	0.6	0.52
ES2b	48.72	15.44	13.96	-37.85	14.01	13.85	0.61	0.53
UK4	55.36	16.66	29.47	-32.92	18.68	13.05	0.61	0.54
MACC (NA)	52.7	25.95	23.13	-23.69	15.46	12.14	0.64	0.45
CA2f	45.88	32.47	7.21	-4.55	13.59	8.64	0.59	0.48
CA2	46.52	32.5	8.69	-4.46	13.88	8.64	0.59	0.48
US6	48.94	30.79	14.04	-9.84	11.6	10.45	0.75	0.49
US7	51.64	28.86	20.35	-15.56	17.28	10.46	0.55	0.46
US8	40.64	25.06	-5.21	-26.4	11.64	12.38	0.64	0.53

performance metrics for all the models, focusing on winter and summer midday periods. In the EU case, the MACC re-analysis consistently underestimates CO surface concentrations, particularly in winter, and this behavior is mimicked by all the models. The fact that the MACC re-analysis shows only small biases at the background station Mace Head near the western domain boundary suggests that this underestimation within the domain is not caused by underestimated background concentrations. Instead, it is likely that CO emissions within the model domain are significantly underestimated both in the MACCity and the TNO/MACC emission inventories especially during winter (see Stein et al. (2014) for a more thorough discussion). Potential discrepancies in the spatial scales represented by the observations and model predictions are likely not a major factor because the analysis focuses on rural sites. In the NA case the underestimation is less severe for MACC. The regional models do not track CO from MACC as closely as in the EU case, suggesting larger differences between the MACCity and the NA emission inventories (see also Section 4.3 below). In fact, the regional models even tend to overestimate CO suggesting an overcompensation of the too low BC by too high CO emissions within the domain. The study of Miller et al. (2008) using tall-tower and aircraft measurements in a model-data assimilation framework indeed indicated that CO emissions over North America as reported by the U.S. EPA might be too high.

4.1.3. NO and NO₂

Nitrogen oxides (NO and NO₂, or NO_x) are major precursors for O₃ and nitrate aerosols. NO_x emissions and their oxidation products strongly influence the concentrations of air pollutants (O₃, PM) (Seinfeld and Pandis, 2006).

For the year 2010, 211 rural stations reported observations for NO and 285 for NO₂ in Europe, while only 15 rural stations for NO and 59 for NO₂ were available in North America. While measurements at rural sites are expected to be better comparable to the coarse resolution model outputs, it should be noted that standard

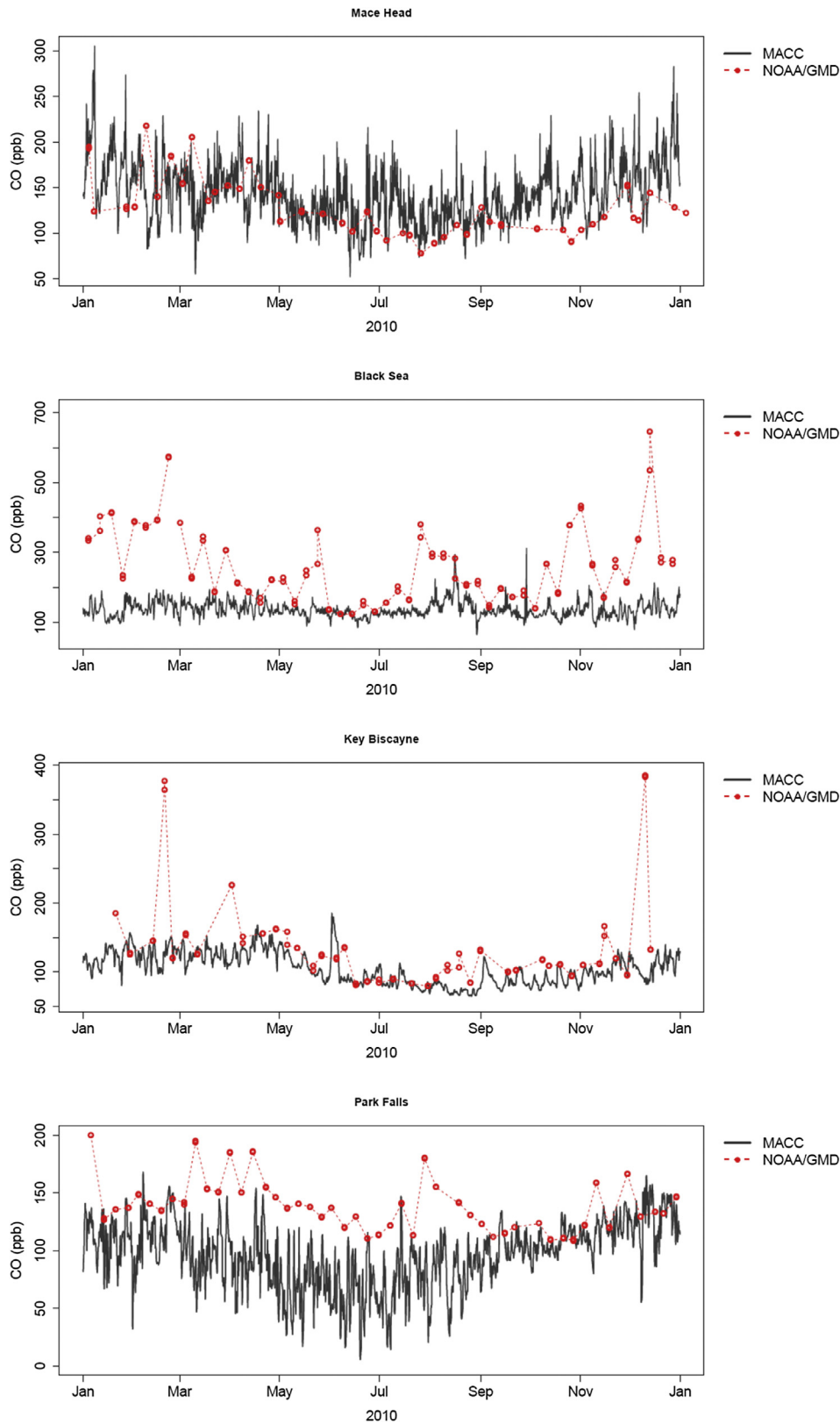


Fig. 3. 2010 time series of mean CO concentrations from the MACC model (black line) and from NOAA/GMD ground-based measurements (red points) at Mace Head, Black Sea, Key Biscayne and Park Falls stations. (For interpretation of the references to colour in this figure legend, the reader is referred to the web version of this article.)

NO₂ measurements based on molybdenum converters can be significantly positively biased at rural sites due to interferences from other oxidized nitrogen species including PAN and HNO₃ (see

for example [Steinbacher et al. \(2007\)](#) and references therein).

[Figs. 5 and 6](#) show the midday median monthly surface concentrations of NO and NO₂ respectively. In [Table 5](#) we report

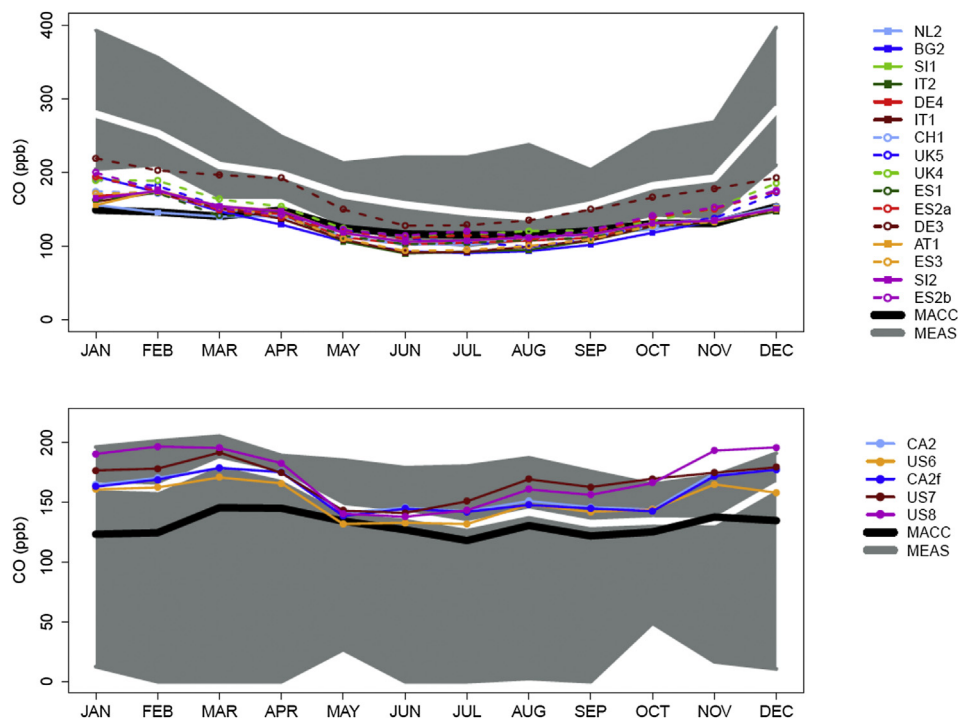


Fig. 4. Time series for 2010 of median monthly CO concentrations, midday values, for EU (top, 12–14 UTC) and NA (bottom, 19–21 UTC) domains. The gray shaded area is the interquartile range of the distribution of observations across all selected stations. The white line represents the median of the observations.

Table 4

Seasonal (summer and winter) midday model performance metrics for CO at ground stations.

Model	CO							
	Mean (ppb)		NMB (%)		RMSE (ppb)		r	
	S	W	S	W	S	W	S	W
MACC (EU)	117.19	150.91	−32.00	−53.12	141.85	306.80	0.13	0.19
BG2	93.09	166.89	−45.89	−48.14	152.82	296.80	0.14	0.21
NL2	106.62	150.42	−38.32	−53.25	149.64	305.42	0.07	0.23
DE3	132.67	203.43	−23.19	−36.78	139.26	278.64	0.09	0.22
UK5	105.51	175.38	−38.69	−45.47	147.43	289.45	0.09	0.26
AT1	111.01	153.74	−35.58	−52.27	146.93	304.07	0.09	0.22
DE4	107.51	156.72	−37.60	−51.33	148.46	302.55	0.09	0.21
ES1	107.69	155.41	−37.50	−51.72	148.17	303.30	0.09	0.21
ES3	98.51	157.62	−42.83	−51.05	152.40	301.77	0.08	0.22
IT1	96.37	154.36	−44.04	−51.11	153.76	300.87	0.07	0.21
IT2	94.91	154.41	−44.88	−50.55	154.58	301.03	0.08	0.21
SI1	111.08	156.60	−35.53	−51.37	147.11	302.43	0.09	0.22
SI2	110.61	156.41	−35.80	−51.43	147.03	302.56	0.09	0.22
CH1	110.26	167.84	−35.98	−47.80	151.80	296.95	0.03	0.19
ES2a	113.86	177.61	−33.86	−44.91	142.34	287.87	0.17	0.27
ES2b	117.65	178.97	−31.64	−44.46	141.45	287.41	0.15	0.27
UK4	126.68	198.61	−27.56	−38.37	179.44	274.32	0.05	0.32
MACC (NA)	123.06	127.59	−2.68	−8.16	109.74	125.63	0.3	0.32
CA2f	167.7	189.57	36.5	37.12	184.57	172.56	0.16	0.05
CA2	169.84	192.94	38.24	39.58	185.18	176.63	0.16	0.05
US6	145.21	170.43	16.66	23.22	119.97	159.91	0.2	0.05
US7	159.48	192.56	27.49	38.96	115.22	158.97	0.34	0.06
US8	164.81	198.89	32.35	43.44	139.74	155.7	0.27	0.13

performance metrics for all the models, focusing on winter and summer midday periods, for combined NO_x .

In both the EU and NA case, the MACC model consistently underestimates the surface NO and NO_2 concentrations throughout the year 2010. The regional models are closer to the observations than the MACC re-analysis, especially for NO_2 . There is significant

spread between the models, especially during winter, indicating substantial inter-model differences in aspects such as vertical mixing, deposition, and chemical lifetimes which warrant further investigation in future diagnostic model evaluation studies. Significantly higher NO_x concentrations are simulated by model ES2a/b as compared to other models in winter, which may be due to the missing heterogeneous reaction of N_2O_5 to HNO_3 in this model which is an important sink of NO_x at nighttime and in winter (Badia and Jorba, 2015).

Anthropogenic, biomass burning, and soil decay NO_x emissions are primarily released within the atmospheric planetary boundary layer (PBL) where the lifetime of NO_x is a few hours in summer and up to one day in winter (Schaub et al., 2007). Given such a short lifetime, the ability of the models to reproduce NO and NO_2 surface values is not directly affected by the MACC boundary conditions, but the consistent underestimation of NO_2 by most models probably indicates a lack of emissions in the inventories used by both the regional models and the MACC re-analysis. On the other hand, since we are looking at rural, relatively emissions-poor locations, the underestimation can be due to other factors as well including an underestimation of the chemical lifetime of NO_x , too high dry deposition, an underestimation of natural emissions from soils as suggested by Jaeglé et al. (2005), or the missing source from lightning in the regional models which, however, would mainly affect the results in summer. Knote et al. (2015) investigated differences between the chemical mechanisms used in the AQMEII-2 models and found differences in simulated radical concentrations of up to 40% for OH and >100% for NO_3 which would indicate a large spread in chemical lifetimes between the models but based on their study it is not possible to conclude on a general positive or negative bias.

Another likely contribution to the model underestimation is a systematic positive bias of the NO_2 measurements. Standard air pollution monitors use molybdenum converters which are known to be cross-sensitive to other reactive nitrogen species including

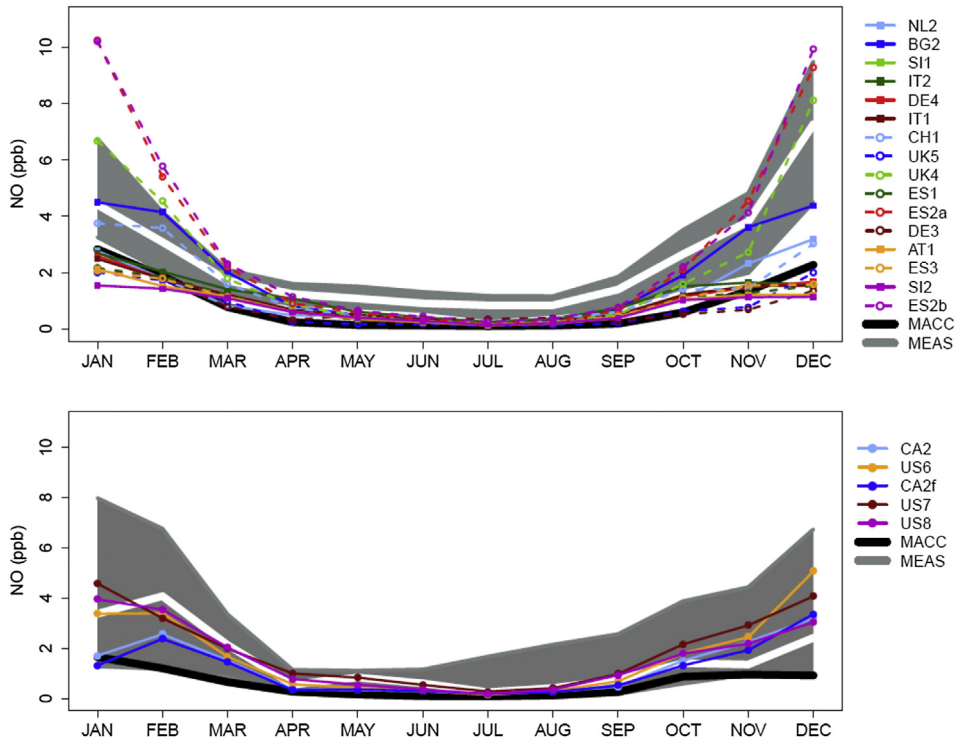


Fig. 5. Time series for 2010 of median monthly NO concentrations, midday values, for EU (top, 12–14 UTC) and NA (bottom, 19–21 UTC) domains. The gray shaded area is the interquartile range of the distribution of observations across all selected stations. The white line represents the median of the observations.

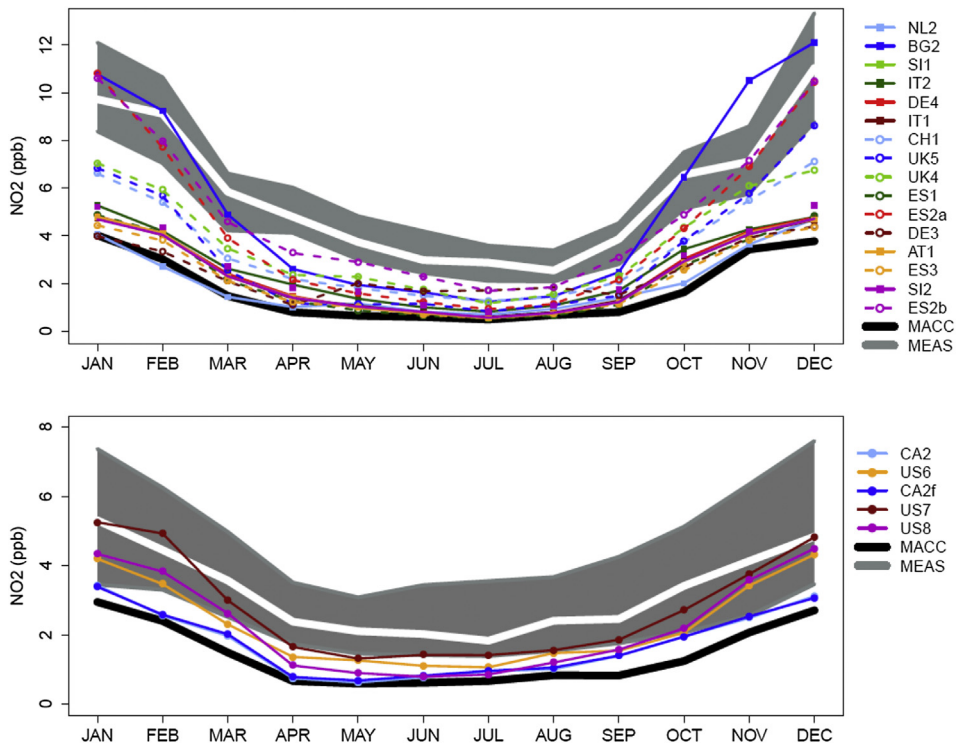


Fig. 6. Time series for 2010 of median monthly NO₂ concentrations, midday values, for EU (top, 12–14 UTC) and NA (bottom, 19–21 UTC) domains. The gray shaded area is the interquartile range of the distribution of observations across all selected stations. The white line represents the median of the observations.

PAN and HNO₃. Steinbacher et al. (2007) found that NO₂ measurements at a rural site in Switzerland from a standard instrument had a rather constant bias of 1.5–2 ppb when compared to an

accurate, NO₂-specific instrument throughout the year. They concluded that only 70–83% of the actually measured NO₂ signal of the molybdenum-based NO_x monitor was attributable to real NO₂.

Table 5
Seasonal (summer and winter) midday model performance metrics for NO_x at ground stations.

Model	NO _x							
	Mean (ppb)		NMB (%)		RMSE (ppb)		r	
	S	W	S	W	S	W	S	W
MACC	0.95	7.32	-76.73	-45.64	4.47	12.69	0.15	0.31
BG2	2.19	13.57	-46.22	0.58	3.94	11.09	0.24	0.42
NL2	1.43	6.6	-65.04	-51.11	4.21	12.82	0.17	0.37
DE3	2.49	5.58	-38.85	-58.69	3.87	13.46	0.18	0.35
UK5	1.34	8.11	-67.24	-39.83	4.28	11.95	0.24	0.41
AT1	1.28	6.06	-68.64	-55.04	4.35	13.23	0.19	0.33
DE4	1.3	6.53	-68.1	-51.56	4.36	12.91	0.18	0.35
ES1	1.19	6.13	-70.77	-54.46	4.49	13.18	0.15	0.33
ES3	1.27	5.87	-68.8	-56.42	4.35	13.27	0.17	0.36
IT1	1.38	6.25	-66.02	-52.33	4.28	13.04	0.18	0.35
IT2	1.87	6.57	-54.06	-48.38	4.06	12.8	0.19	0.36
SI1	1.35	5.82	-67.02	-56.79	4.34	13.35	0.18	0.34
SI2	1.31	5.73	-67.75	-57.42	4.32	13.37	0.19	0.35
CH1	2.44	10.57	-38.3	-21.6	9.7	11.43	0.05	0.39
ES2a	2.15	17.14	-47.06	26.81	4.71	14.65	0.14	0.35
ES2b	2.63	17.69	-35.2	30.94	5	14.68	0.13	0.36
UK4	2.44	13.31	-40.04	-1.47	4.42	12.23	0.21	0.41
MACC	0.9	4.89	-74.73	-52.53	4.4	11.66	0.29	0.42
CA2f	2.35	7.24	-33.51	-29.4	4.6	11.14	0.26	0.46
CA2	2.31	7.66	-34.52	-25.24	4.58	11.21	0.27	0.47
US6	2.37	10.69	-29.06	9.29	3.76	11.29	0.37	0.51
US7	2.57	12.3	-23.55	23.27	3.47	12.45	0.42	0.44
US8	2.29	10.52	-30.86	6.75	4.38	12.53	0.24	0.39

4.1.4. SO₂ and SO₄²⁻

SO₂ is a major atmospheric pollutant of mainly anthropogenic origin, produced by the combustion of fossil fuel and by industrial facilities. With an average lifetime in the troposphere of few days (Lee et al., 2011), SO₂ is oxidized to form sulfuric acid and sulfate aerosols. SO₂ is the principal precursor of sulfate aerosols and,

because of its links to climate, air quality and human health issues, is extensively and continuously monitored on a global scale.

Fig. 7 shows the midday median monthly SO₂ surface concentrations averaged over 165 (EU) and 44 (NA) rural stations. In Table 6 we report performance metrics for all the models. In the EU case, the MACC re-analysis overestimates the surface SO₂ concentrations during the winter season (up to 2 ppbv with respect to the median of the observations), while it reproduces the measurements well during the rest of the year. Flemming et al. (2014) suggested that the overestimation in winter and the correspondingly too large amplitude of the seasonal cycle could be introduced by the diffusion scheme in IFS-MOZART. The seasonal bias is much reduced in the new model version C-IFS which, however, not only differs from IFS-MOZART with respect to vertical mixing, but also with respect to sulfur chemistry and wet and dry deposition. In the NA case, the MACC re-analysis is within the interquartile range of the observations for most of the year, but shows a pronounced seasonal cycle not seen in the observations that manifests itself in a tendency to underestimate surface SO₂ in summer. Due to its rather short lifetime, SO₂ does not get transported efficiently from the borders towards the center of the domain, where the performance of the models is not strongly affected by the MACC re-analysis biases. In winter, the regional models show significantly lower SO₂ concentrations than the MACC re-analysis, more consistent with the observations. However, over NA the regional models also exhibit a seasonal cycle that is not visible in the observations. Some models show a significant underprediction, notably UK5 over EU. Over NA, CA2 and CA2f show much higher SO₂ than all other models and significantly overpredict SO₂ in winter. The reasons for these model-to-model differences as well as the differences between the observed and simulated seasonal cycles over NA should be investigated further in future studies.

Sulfate is produced by oxidation from SO₂ in both the gas phase and the liquid phase. Oxidation in the gas phase by OH is more

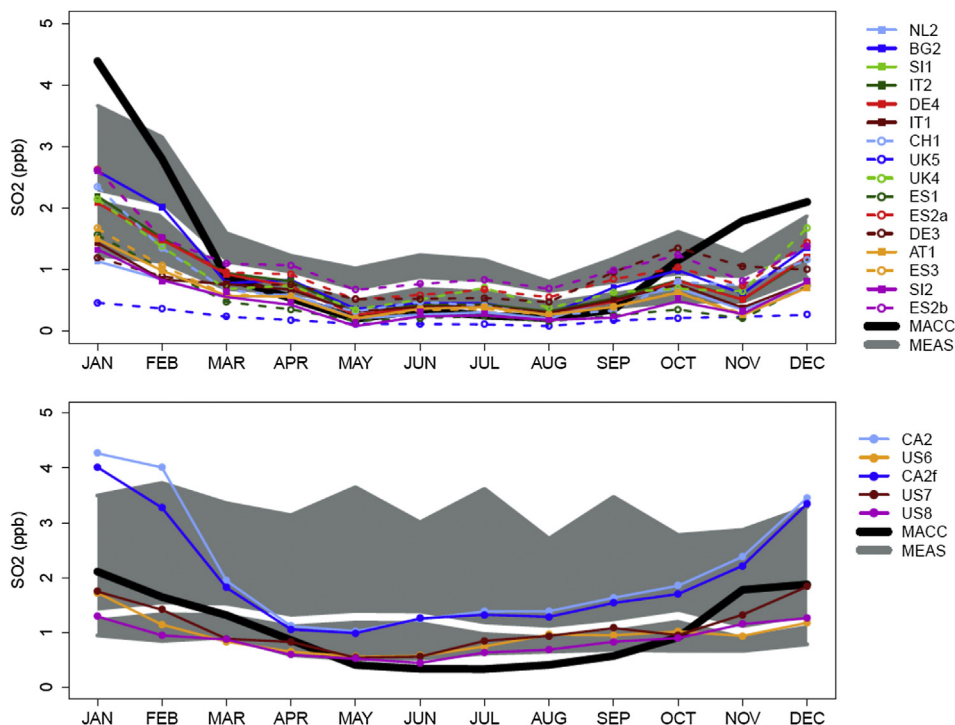


Fig. 7. Time series for 2010 of median monthly SO₂ concentrations, midday values, for EU (top, 12–14 UTC) and NA (bottom, 19–21 UTC) domains. The gray shaded area is the interquartile range of the distribution of observations across all selected stations. The white line represents the median of the observations.

Table 6Seasonal (summer and winter) midday model performance metrics for SO₂ at ground stations.

Model	SO ₂							
	Mean (ppb)		NMB (%)		RMSE (ppb)		r	
	S	W	S	W	S	W	S	W
MACC (EU)	0.32	2.56	-63.48	39.89	2.34	3.03	0.1	0.49
BG2	0.55	1.66	-36.74	-9.06	2.17	2.77	0.34	0.5
NL2	0.38	0.82	-56.45	-54.9	2.23	3.08	0.3	0.4
DE3	0.64	0.96	-27.13	-47.51	2.21	3.06	0.27	0.39
UK5	0.2	0.42	-76.76	-77	2.29	3.34	0.34	0.28
AT1	0.48	0.86	-44.74	-53.11	2.19	2.99	0.32	0.45
DE4	0.5	1.24	-43	-31.92	2.19	2.92	0.32	0.42
ES1	0.33	0.91	-61.78	-50.35	2.23	2.97	0.33	0.45
ES3	0.47	0.94	-46.32	-48.49	2.19	2.97	0.32	0.44
IT1	0.52	0.89	-40.48	-50.96	2.18	2.99	0.33	0.46
IT2	0.53	1.25	-39.13	-31.3	2.18	2.93	0.32	0.43
SI1	0.37	0.79	-57.59	-56.69	2.22	3.02	0.32	0.45
SI2	0.36	0.79	-58.61	-56.77	2.22	3.02	0.32	0.45
CH1	0.67	1.59	-24.11	-12.83	2.27	2.91	0.24	0.41
ES2a	0.73	1.55	-16.59	-14.93	2.17	2.88	0.32	0.45
ES2b	0.77	1.42	-12.4	-22.02	2.18	2.92	0.31	0.43
UK4	0.74	1.65	-15.38	-9.78	2.26	3.07	0.3	0.46
MACC (NA)	0.42	2.38	-81.25	-13.96	5.67	7.15	0.16	0.19
CA2f	2.52	3.64	12.34	33.71	5.32	7.38	0.34	0.27
CA2	2.54	3.86	13.04	41.63	5.34	7.49	0.34	0.27
US6	1.4	1.91	-29.24	-31.66	4.6	6.94	0.41	0.41
US7	1.47	2.12	-26.06	-25.71	4.6	6.91	0.4	0.42
US8	1.16	1.7	-37.99	-38.71	4.74	7.11	0.36	0.38

important during the summer compared to other seasons. Note that in the MACC model there are two representations of SO₂ and sulfate, one from the mainly gas-phase chemistry of MOZART, and one from the MACC aerosol module (Morcrette et al., 2009) based on a simple SO₂ to sulfate conversion approach. The fields provided as BC for the regional models were SO₂ from the MOZART scheme

but sulfate from the MACC aerosol module. Different from the regional models, the SO₂ and sulfate fields analyzed for the MACC re-analysis are thus not chemically coupled. The sulfate component of particulate matter is overestimated during summer by the MACC re-analysis both in EU and NA, as shown in Fig. 8, where we present daily averaged median monthly sulfate aerosol surface concentrations, averaged over 33 (EU) and 70 (NA) rural stations.

Performance metrics for all the models are reported in Table 7. For the EU case, the measurements are reported as PM₁₀ (SO₄²⁻) but in NA as PM_{2.5} (SO₄²⁻). One possible reason for the positive bias in the MACC re-analysis in the summer months is that the MACC aerosol model does not contain a representation of ammonium nitrate aerosol which represents a large component of the European aerosol loading. Therefore the assimilation of satellite AOD will tend to increase the other aerosol components to give the correct AOD overall. In the EU case (top panel), model CH1 follows closely the MACC re-analysis predictions and shows a similar strong positive bias pattern. This overestimation contrasts with the findings of a previous evaluation of COSMO-ART (Knote et al., 2011) which suggested under-rather than over-prediction of sulfate. This is probably due to the implementation of a comprehensive wet chemistry scheme (Knote and Brunner, 2013) that had not been included in the previous evaluation. The other regional models do not show the same positive bias as MACC and COSMO-ART, indicating that the sulfate simulations are not very sensitive to the choice of chemical boundary conditions, but further analysis is needed to investigate the relative role of long-range transport vs. within-domain formation in simulating regional-scale sulfate. The underestimation of sulfate in winter by a number of models is likely related to an underestimation of SO₂ to sulfate oxidation in clouds as also noted by Im et al. (2015a,b) or missing heterogeneous oxidation of SO₂ as reported in Wang et al. (2015). Balzarini et al. (2015) investigated the in-cloud oxidation pathway in more detail for two different versions of WRF-Chem with (SI2) and without (IT1) SO₂ oxidation in cloud

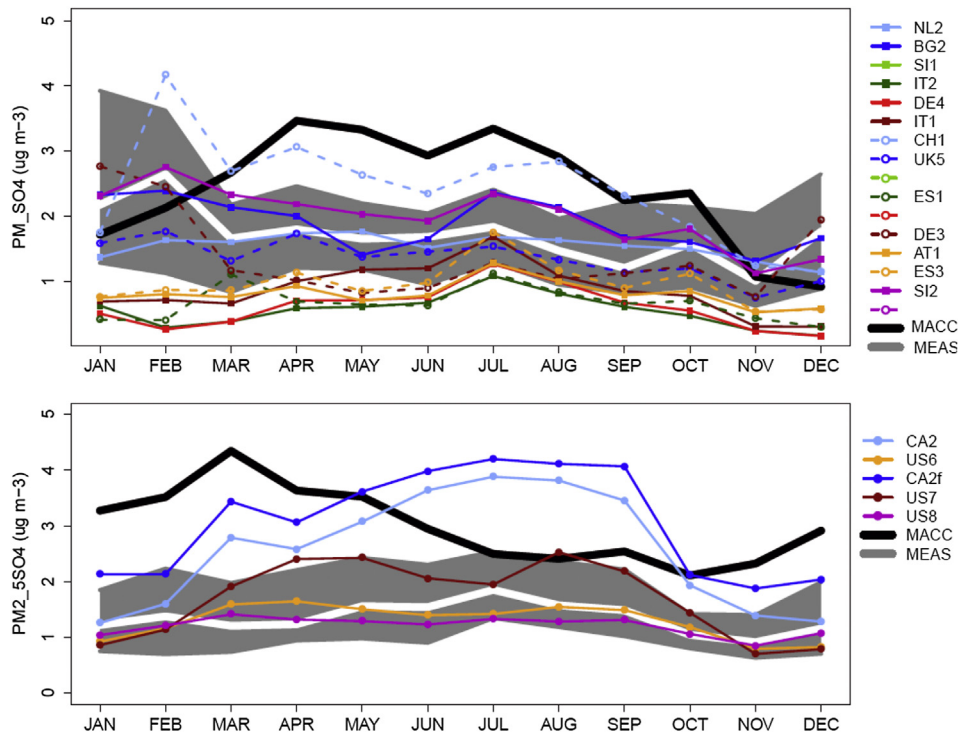


Fig. 8. Top panel: time series for 2010 of median monthly PM₁₀-SO₄ concentrations for EU. Bottom panel: time series for 2010 of median monthly PM_{2.5}-SO₄ concentrations for NA. The gray shaded area is the interquartile range of the distribution of observations across all selected stations. The white line represents the median of the observations.

Table 7
Seasonal (summer and winter) daily model performance metrics for SO₄²⁻ at ground stations.

Model	SO ₄ ²⁻							
	Mean (ppb)		NMB (%)		RMSE (ppb)		r	
	S	W	S	W	S	W	S	W
MACC (EU)	3.19	1.7	89.13	-29.37	2.56	2.54	0.43	0.41
BG2	1.94	2.28	15.59	-5.46	1.26	2.11	0.59	0.57
NL2	1.77	1.35	5.64	-44.13	1.56	2.61	0.39	0.36
DE3	1.15	2.28	-28.72	-5.72	1.29	2.18	0.55	0.54
UK5	1.54	1.62	-8.33	-32.88	1.37	2.36	0.44	0.49
AT1	1.11	0.78	-34.22	-67.82	1.31	2.74	0.52	0.55
DE4	1.07	0.36	-36.08	-84.97	1.33	3.22	0.51	0.2
ES1	0.95	0.42	-43.14	-82.62	1.4	3.1	0.47	0.42
ES3	1.5	0.8	-11.01	-66.97	1.42	2.73	0.5	0.53
IT1	1.46	0.65	-13.4	-72.92	1.42	2.95	0.47	0.36
IT2	0.91	0.38	-45.68	-83.1	1.39	3.2	0.52	0.2
SI1	2.22	2.16	31.67	-10.24	1.74	2.21	0.45	0.57
SI2	2.22	2.16	31.53	-10.29	1.75	2.21	0.45	0.57
CH1	2.87	2.21	67.06	-8.37	2.13	2.46	0.4	0.46
MACC (NA)	2.84	3.02	48.19	130.85	1.75	2.85	0.58	0.44
CA2f	4.48	2.07	132.31	52.64	4.06	1.53	0.65	0.64
CA2	4	1.49	107.91	12.36	3.45	1.14	0.68	0.6
US6	1.62	1.01	-15.58	-23.16	0.99	0.89	0.82	0.68
US7	2.34	0.91	20.91	-29.98	1.23	1.18	0.73	0.33
US8	1.64	1.53	-14.8	14.98	1.12	1.4	0.77	0.68

water. The model IT1 indeed is one of the models that strongly underestimate sulfate in winter while SI2 is rather closely following the observations. Although the other WRF-Chem models did include aqueous phase chemistry, they follow more closely the seasonal

profile of IT1 than the profile of SI2. However, these models used different modules for both aqueous chemistry and wet deposition than SI2. A further analysis of the impact of different configurations available in WRF-Chem on SO₂ and sulfate would thus be highly valuable.

Using a diagnostic analysis approach, Wang et al. (2015) investigated several possible factors contributing to the under-predictions of sulfate in the US. They found that model performance for sulfate can be improved by the use of a more detailed convective cloud chemistry, addition of SO₂ heterogeneous chemistry, and the use of a more realistic surface wind drag parameterization, among which the addition of SO₂ heterogeneous chemistry contributes the most to the improvement.

The models UK5 and NL2 also represent sulfate concentrations fairly accurately and at the same time are among the models with rather low SO₂ concentrations in winter (especially UK5), suggesting a more efficient SO₂ to sulfate conversion as compared to other models.

In the NA case (bottom panel of Fig. 8), CA2 and CA2f show a similar pattern of strong positive bias, similarly to SO₂, but with the largest overestimation in summer, as opposed to winter for SO₂. The other models are able to well reproduce sulfate surface concentrations, but this pattern is not correlated with the positive bias shown by the MACC re-analysis.

4.2. Vertical profiles at Frankfurt airport

Most air pollutants have a longer lifetime at higher altitudes and show a much smoother distribution than in the boundary layer.

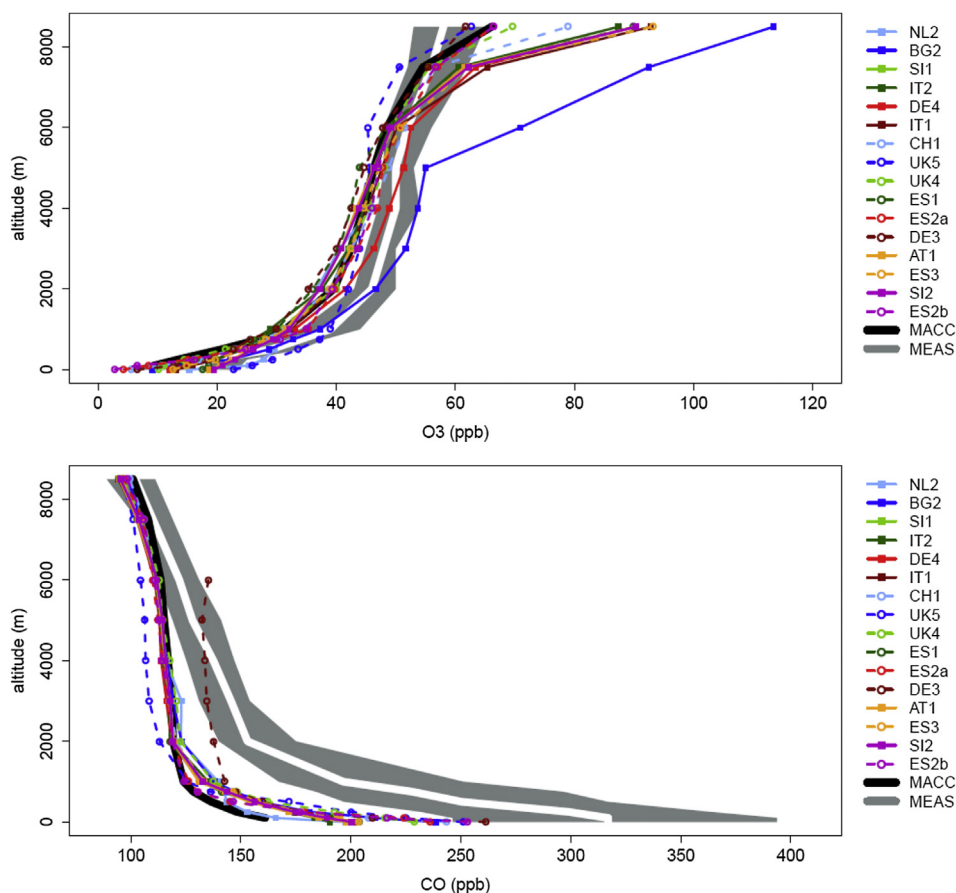


Fig. 9. 2010 winter vertical profiles of median O₃ (top) and CO (bottom) concentrations at Frankfurt airport. The gray shaded area is the interquartile range of the distribution of observations across all selected stations. The white line represents the median of the MOZAIC observations.

This is a consequence of slower photochemistry due to generally lower concentrations and lower temperatures and the absence of emission sources and (dry) deposition sinks. Therefore, the influence of the MACC re-analysis is expected to be larger in the free and upper troposphere than in the boundary layer.

In Fig. 9, we show the winter averaged vertical profiles at Frankfurt airport for O₃ (top panel) and CO (bottom panel), in which all regional models and the MACC re-analysis are compared to MOZAIC aircraft measurements.

Despite the large spread at the surface, O₃ concentrations in the models are similar in the lower troposphere and start to diverge again above 6 km. While most models used a vertical resolution between 30 and 40 levels in their simulations (Brunner et al., 2015), the spacing of these levels in the tropopause region varies between models and may affect the downward mixing of stratospheric ozone into the upper troposphere. However, the two simulations performed with the NMMB-BSC model at two largely differing

vertical resolutions (ES2a: 24 levels, ES2b: 48 levels), differ only little in the upper troposphere, indicating that factors other than vertical resolution must dominate these results such as differences in the treatment of ozone in the stratosphere or different vertical model tops. Note that due to the lack of observations in spring and summer, the profiles are only representative of the situation in fall and winter. In these seasons, O₃ shows a pronounced vertical profile with low values near the surface possibly influenced by the titration of O₃ by NO. Above the PBL the regional models quite closely track the MACC re-analysis, indicating a larger influence of BC at higher altitudes, though as noted above the spread between the regional models begins to increase in the upper troposphere.

Over Frankfurt, CO concentrations are severely underestimated up to ~6 km, with a bias close to the surface exceeding 200 ppb. All the models, except for DE3 and UK5, follow closely the vertical profile of the MACC re-analysis, with an increasing spread towards the surface. This result is consistent with the analysis of CO

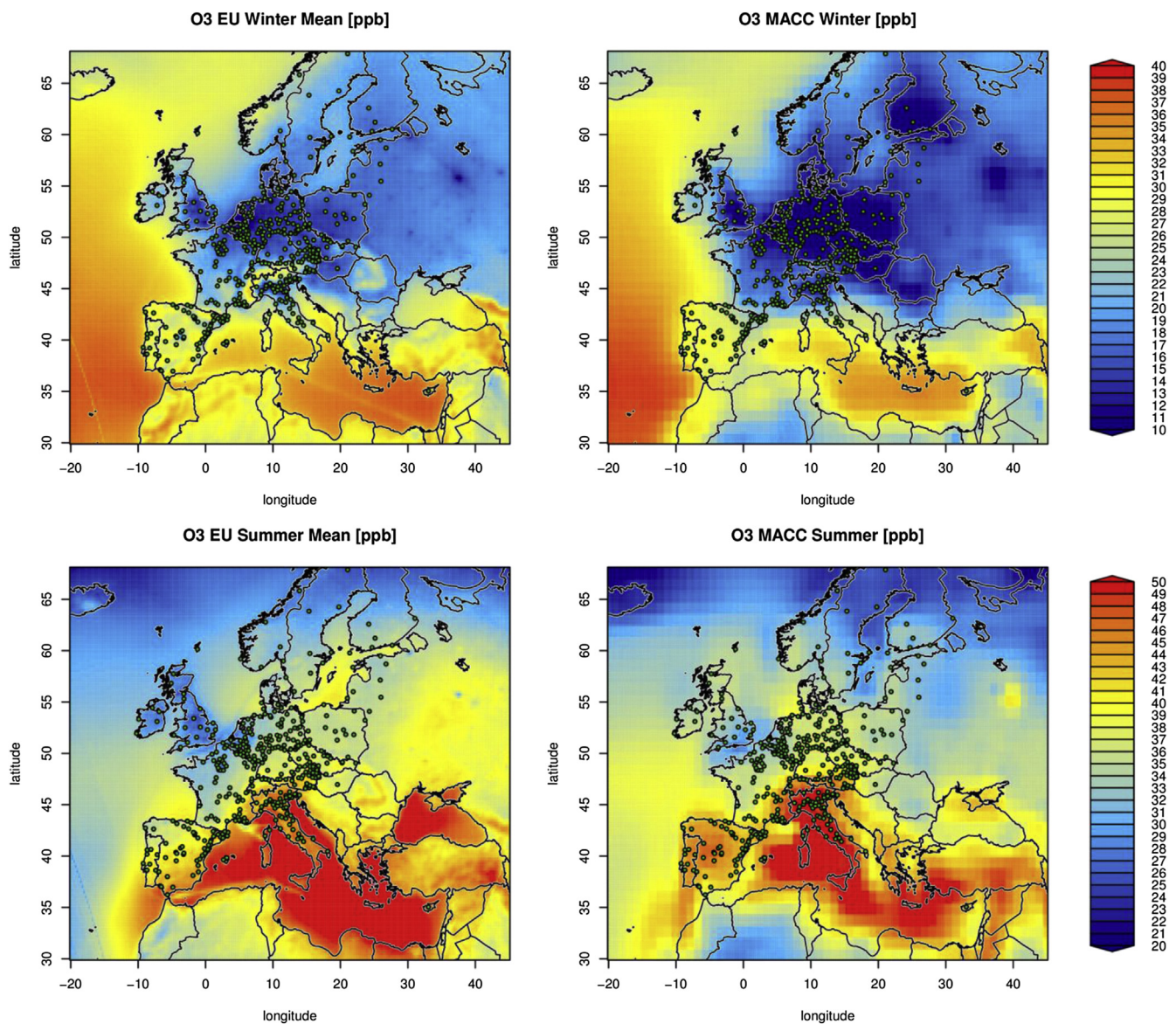


Fig. 10. Winter (top panels) and summer (bottom panels) surface 2010 means for O₃ in the EU case. Right: MACC re-analysis. Left: Average over the 16 regional models that simulated the EU case. The superposed green dots on the maps represent the ground stations selected for the analysis at receptor points. Stripes near the domain borders are due to the different model domains of the regional models leading to a varying number of models contributing to the mean. (For interpretation of the references to colour in this figure legend, the reader is referred to the web version of this article.)

concentrations at ground stations and suggests that the emission inventories used by the MACC re-analysis and the regional models might be the cause of large negative biases closer to the surface, in particular at urban and polluted sites. It further suggests that CO concentrations in the free troposphere are quite closely tied to the concentrations of the model providing the boundary conditions. The deviations of the models DE3, UK5 and BG2 from the general behavior may point at problems with the technical implementation of the chemical boundary conditions in these models.

4.3. Spatial analysis of CO and O₃

Due to simulation strategy and resources available, all the participating regional modeling groups only performed one simulation for the year 2010 using the same BC. The lack of sensitivity simulations with alternate sets of BC precludes us from quantitatively determining the effect of boundary conditions on the simulation results. Nevertheless, it is possible to qualitatively

demonstrate the influence of the use of the MACC re-analysis as BC, in particular by analyzing CO concentrations, the longest-lived species simulated and delivered as a gridded field by all models.

In Figs. 10 and 11 we show the winter and summer average surface concentrations over EU for O₃ and CO, respectively. The superposed green dots represent the ground stations selected for the analysis in Section 4.1.1 and 4.1.2. These maps show clearly the difference in emissions between the models and the MACC re-analysis: While the CO concentrations in the regional models are similar to MACC near the domain borders, they are significantly higher over the European continent in winter. Emissions outside of Europe were missing in the TNO/MACC inventory resulting in a strong underestimation of CO concentrations over North Africa, especially over Cairo. Although the MACC re-analysis and the regional models used different forest fire emission inventories (MACC: GFAS (Kaiser et al., 2012), regional models: IS4FIRES (Sofiev et al., 2009)), the CO concentrations over the Russian forest fire regions in summer are quite similar though

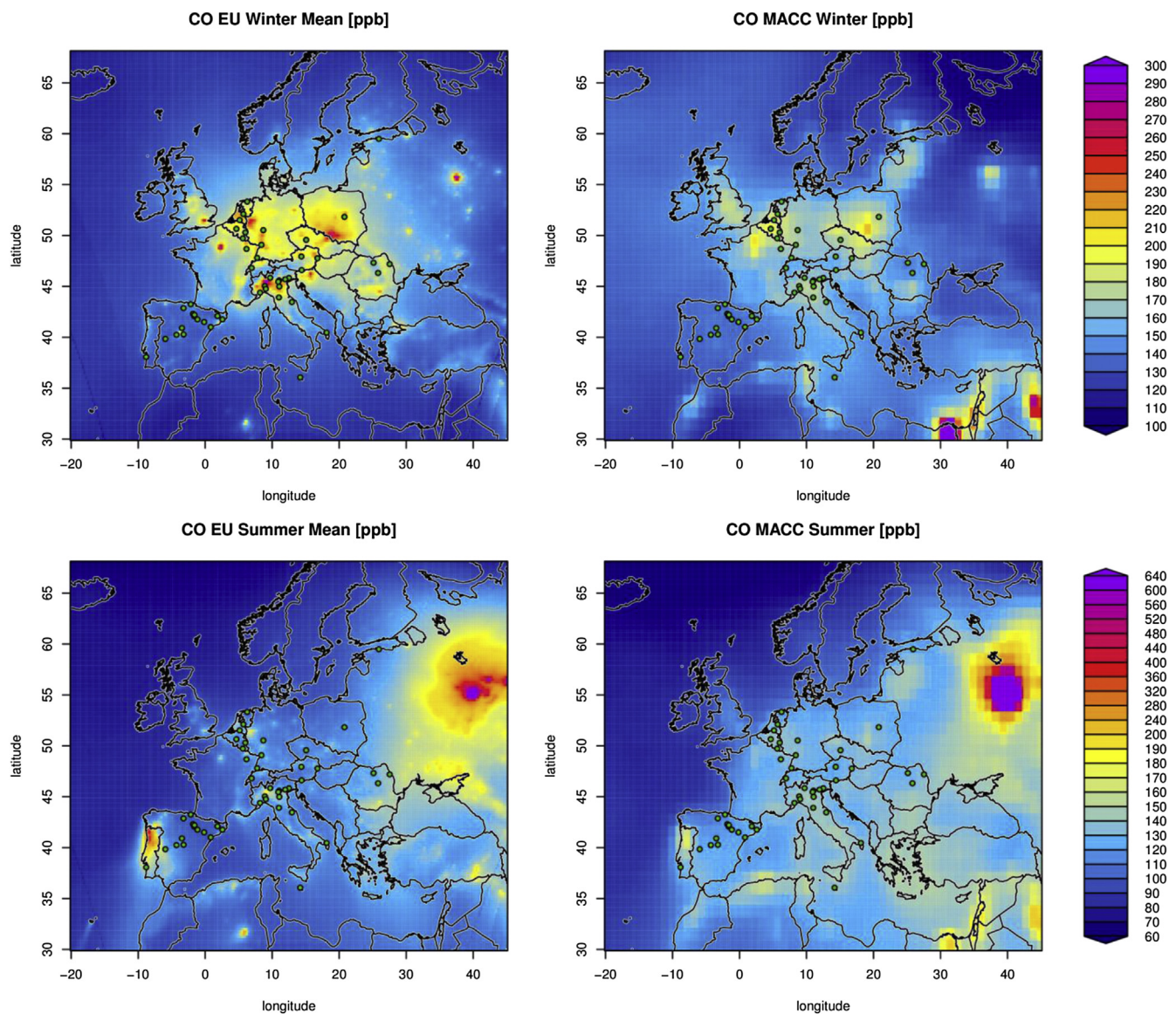


Fig. 11. Winter (top panels) and summer (bottom panels) surface 2010 means for CO in the EU case. Right: MACC re-analysis. Left: Average over the 16 regional models that simulated the EU case. The superposed green dots on the maps represent the ground stations selected for the analysis at receptor points. Stripes near the domain borders are due to the different model domains of the regional models leading to a varying number of models contributing to the mean. (For interpretation of the references to colour in this figure legend, the reader is referred to the web version of this article.)

somewhat higher in MACC. O_3 concentrations in the regional models are also similar to MACC near the domain borders, but over continental Europe the differences become larger. This is especially true for winter where MACC shows much lower O_3 concentrations. As suggested by the analysis in section 4.1.1, this is mostly due to a strong underprediction of ozone at nighttime in the MACC re-analysis. This underestimation could indicate a too stable nocturnal boundary layer which would lead to strong depletion of ozone near the surface by dry deposition. Another reason could be the fact that no diurnal cycle is imposed on NO_x emissions in the IFS-MOZART model which leads to too high emissions at nighttime and correspondingly too strong O_3 titration by NO at night.

These findings confirm our speculation that strong biases in O_3 and CO are to a large extent due to differences in emission inventories between the MACC re-analysis and the regional models.

In Figs. 12 and 13 we show the winter and summer average surface concentrations for O_3 and CO over NA. Again, the

superposed green dots on the maps represent the ground stations selected for the analysis in Section 4.1.1 and 4.1.2. Similar to the EU case, the differences between the regional models and the MACC re-analysis can be quite large within the interior of the domain confirming the importance of the chosen emission inventories even for relatively long-lived species such as CO and ozone. The CO concentrations are much larger in the regional models than in MACC especially in winter, consistent with the findings presented in Section 4.1.2.

The differences in summertime CO concentrations over Canada can be explained by the fact that SMARTFIREv2 covers only the US and no Canadian wildfire emissions were contained in the emission inventories used by the regional models. While ozone concentrations are rather similar in the mean of the regional models and the global model in summer, the MACC re-analysis shows generally much lower O_3 in winter similar to the EU case.

It is important to note that the regional models are run at much

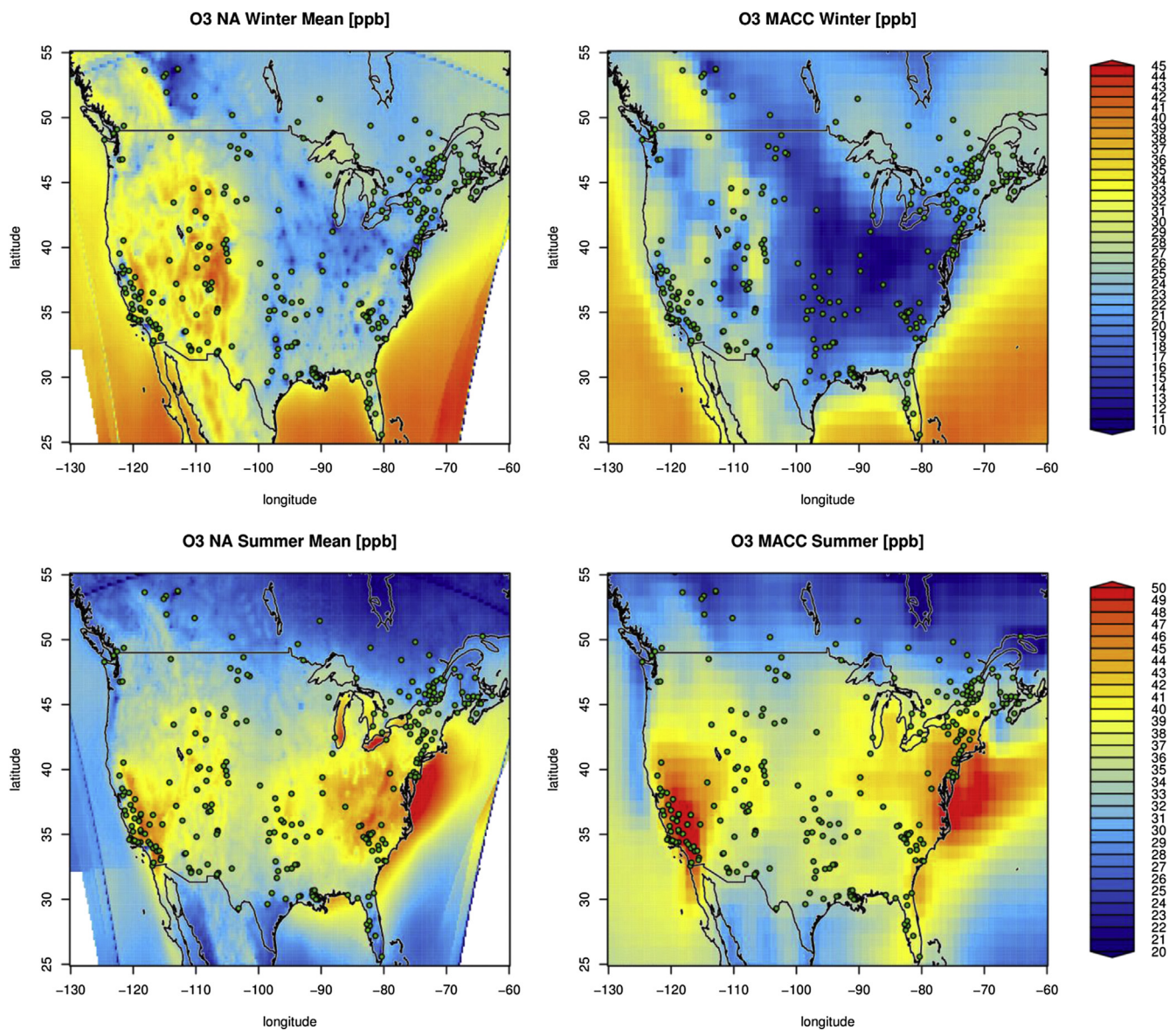


Fig. 12. Winter (top panels) and Summer (bottom panels) surface 2010 means for O_3 in the NA case. Right: MACC re-analysis. Left: Average over the 5 regional models that simulated the NA case. The superposed green dots on the maps represent the ground stations selected for the analysis at receptor points. Stripes near the domain borders are due to the different model domains of the regional models leading to a varying number of models contributing to the mean. (For interpretation of the references to colour in this figure legend, the reader is referred to the web version of this article.)

higher resolution than the MACC re-analysis. As a consequence, the regional models generally show much more small scale structure in the concentrations of O_3 and CO at the surface than the MACC re-analysis. Since there are other factors which could influence the surface concentrations beyond the differences in emission inventories, including the effect of vertical mixing, dry deposition and chemistry schemes, we stress that these differences deserve further analysis.

5. Summary and conclusions

Sixteen European models and five North American models have been used to simulate the year 2010 within AQMEII-2. All models have taken their boundary conditions from the MACC re-analysis of the global IFS-MOZART model. All groups have provided their model outputs regridded on the same horizontal and vertical grids. We have evaluated the MACC re-analysis along with all other

models against a set of ground station observations for O_3 , CO, NO, NO_2 , SO_2 and SO_4^{2-} concentrations.

We have further investigated the ability of all models to reproduce surface O_3 concentrations (see also Im et al., 2015a) and we have looked at midday and midnight values separately. This allowed us to isolate the different performance of the MACC re-analysis in simulating O_3 at different times of the day. Over the EU domain, the MACC re-analysis has a general tendency to underestimate O_3 at midnight. At midday, while there is still an underestimate during the winter season, the MACC re-analysis overestimates O_3 . The general tendency to underestimate O_3 during winter is shown also in vertical profiles. Over the NA domain, the MACC re-analysis shows a good agreement with observations.

The longest lived species analyzed in this study was CO, for which the MACC re-analysis has negative biases over the European domain, mainly due to differences in emission inventories, while at remote NOAA stations near the domain boundaries the MACC re-

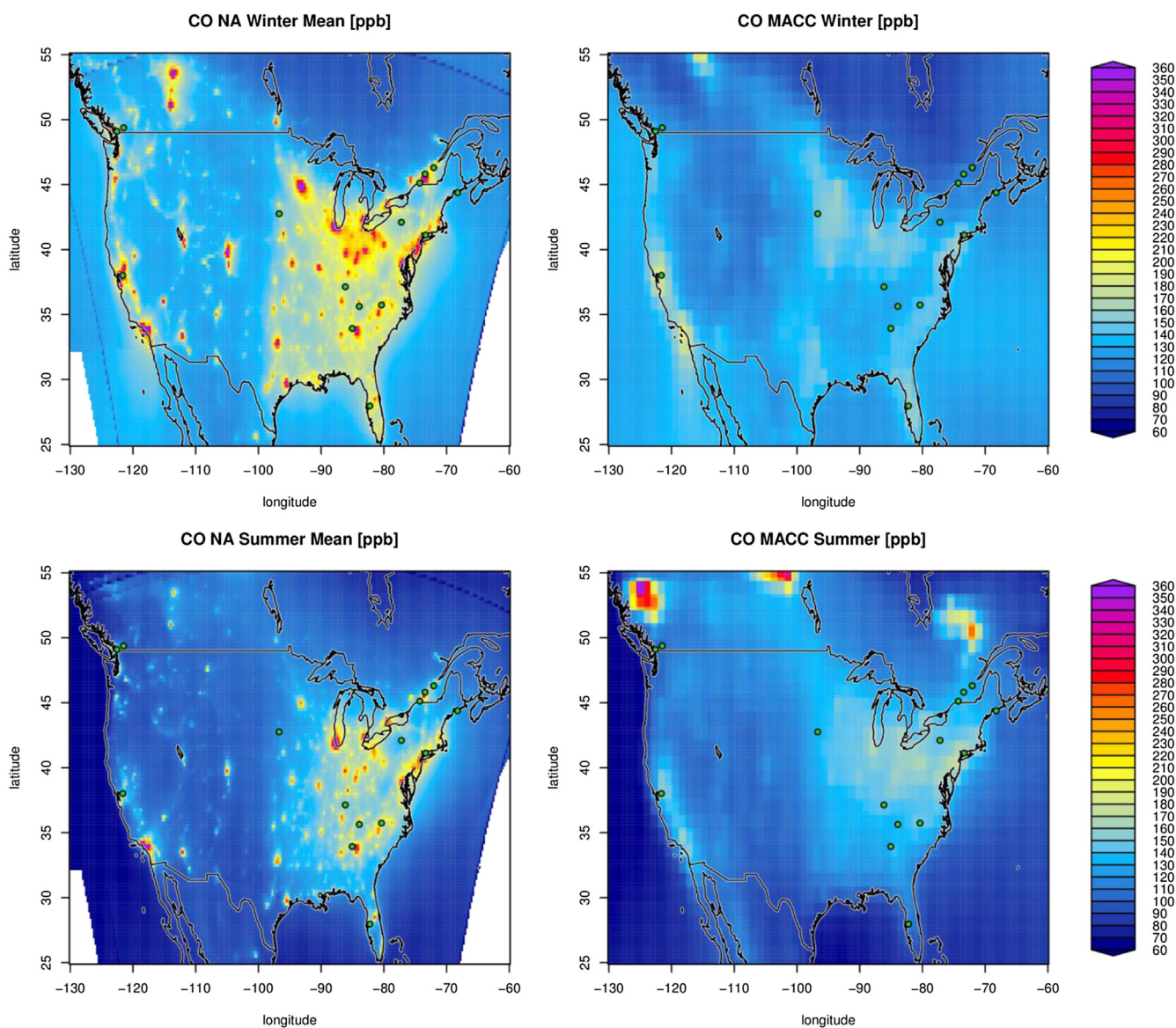


Fig. 13. Winter (top panels) and Summer (bottom panels) surface 2010 means for CO in the NA case. Right: MACC re-analysis. Left: Average over the 5 regional models that simulated the NA case. The superposed green dots on the maps represent the ground stations selected for the analysis at receptor points. Stripes near the domain borders are due to the different model domains of the regional models leading to a varying number of models contributing to the mean. (For interpretation of the references to colour in this figure legend, the reader is referred to the web version of this article.)

analysis well reproduces CO concentrations.

The negative CO bias in the MACC re-analysis is also seen in the regional models at the surface, and in the vertical profile for all models (with the only exception of DE3). The analysis of surface concentrations of CO over the NA domain shows a much better agreement with observations both in the MACC re-analysis and regional model simulations. On the other hand, the regional models are missing wildfire emissions over Canada during 2010 summer season, since SMARTFIREv2 covers only the US and no Canadian wildfire emissions were contained in the emission inventories used by the regional models.

Although sensitivity simulations are crucial for a precise quantification of BC influence on any numerical experiment, from our analysis clearly emerges that biases in the MACC re-analysis are partly traced by the models, depending on the lifetime of the transported species. This influence is most obvious for ozone, where the underestimation in winter in MACC is mimicked by the regional models, while for CO the emissions in the interior of the domain appear to play an equally important role as the boundary conditions. The strong differences in CO between the global and regional simulations are pointing at significant differences in the underlying emission inventories, which calls for a better harmonization of regional and global inventories in the future. For the shorter-lived species NO_x, SO₂ and sulfate, the influence of boundary conditions appears to be minor. The sometimes large differences between the regional models and the MACC-reanalysis as well as among the regional models themselves must be due to other factors. A particularly large spread between models and large differences from observations was found for sulfate, indicating that the conversion of SO₂ to sulfate is often not well represented probably due to a misrepresentation or lack of SO₂ oxidation in cloud water and through heterogeneous reactions on the surface of aerosols.

Acknowledgments

We acknowledge NOAA/ESRL for providing their data through the WDCGG database and making them available for use in research. We gratefully acknowledge the support of the European groups through COST Action ES1004 EuMetChem. Individual authors of this article were additionally supported by the following projects and grants: Lea Giordano through Swiss State Secretariat for Education, Research and Innovation, project C11.0144. O. Jorba is supported by grant SEV-2011-00067 of Severo Ochoa Program awarded by the Spanish Government. The UPM authors thankfully acknowledge the computer resources, technical expertise and assistance provided by the Centro de Supercomputación y Visualización de Madrid (CESVIMA) and the Spanish Supercomputing Network (BSC). Rahela Žabkar and Luka Honzak were supported by the Centre of Excellence for Space Sciences and Technologies SPACE-SI, partly financed by the European Union, European Regional Development Fund and Republic of Slovenia, Ministry of Higher Education, Science, Sport and Culture. Y. Zhang acknowledges funding support from the NSF Earth System Program (AGS-1049200) and computing support from Yellowstone by NCAR's Computational and Information Systems Laboratory, sponsored by the National Science Foundation and Stampede, provided as an Extreme Science and Engineering Discovery Environment (XSEDE) digital service by the Texas Advanced Computing Center (TACC). G. Curci and P. Tuccella were supported by the Italian Space Agency in the frame of PRIMES project (contract n. I/017/11/0). The technical assistance of Bert van Ulft (KNMI) and Arjo Segers (TNO) in producing the results of the NL2 model is gratefully acknowledged. The authors would also like to thank numerous data providers: the ECMW/MACC project & Météo-France/CNRM-GAME for chemical

boundary conditions; the MOZAIC Data Centre and its contributing airlines for aircraft takeoff and landing vertical profiles. The Joint Research Center Ispra/Institute for Environment and Sustainability provided its ENSEMBLE system for model output harmonization and analyses and evaluation. The views expressed here are those of the authors and do not necessarily reflect the views and policies of the U.S. EPA or any other organization participating in the AQMEII project. This paper has been subjected to EPA review and approved for publication.

References

- Badia, A., Jorba, O., 2015. Gas-phase evaluation of the online NMMB/BSC-CTM model over Europe for 2010 in the framework of the AQMEII-Phase2 project. *Atmos. Environ.* 115, 657–669.
- Balzarini, A., Pirovano, G., Honzak, L., Žabkar, R., Curci, G., Forkel, R., Hirtl, M., San José, R., Tuccella, P., Grell, G.A., 2015. WRF-Chem model sensitivity to chemical mechanisms choice in reconstructing aerosol optical properties. *Atmos. Environ.* 115, 604–619.
- Baklanov, A., Schlünzen, K., Suppan, P., Baldasano, J., Brunner, D., Aksoyoglu, S., Carmichael, G., Douras, J., Flemming, J., Forkel, R., Galmarini, S., Gauss, M., Grell, G., Hirtl, M., Joffre, S., Jorba, O., Kaas, E., Kaasik, M., Kallos, G., Kong, X., Korsholm, U., Kurganskiy, A., Kushta, J., Lohmann, U., Mahura, A., Manders-Groot, A., Maurizi, A., Moussiopoulos, N., Rao, S., Savage, N., Seigneur, C., Sokhi, R., Solazzo, E., Solomos, S., Sörensen, B., Tsegas, G., Vignati, E., Vogel, B., Zhang, Y., 2014. Online coupled regional meteorology chemistry models in Europe: current status and prospects. *Atmos. Chem. Phys.* 14 (1), 317–398.
- Brunner, D., Jorba, O., Savage, N., Eder, B., Makar, P., Giordano, L., Badia, A., Balzarini, A., Baro, R., Bianconi, R., Chemel, C., Forkel, R., Jimenez-Guerrero, P., Hirtl, M., Hodzic, A., Honzak, L., Im, U., Knote, C., Kuenen, J., Makar, P., Manders-Groot, A., Neal, L., Perez, J., Pirovano, G., San Jose, R., Savage, N., Schroder, W., Sokhi, R., Syrakov, D., Torian, A., Werhahn, J., Wolke, R., van Meijgaard, E., Yahya, K., Žabkar, R., Zhang, Y., Zhang, J., Hogrefe, C., Galmarini, S., 2014. Comparative analysis of meteorological performance of coupled chemistry-meteorology models in the context of AQMEII phase 2. *Atmos. Environ.* 115, 470–498.
- Dennis, R., Fox, T., Fuentes, M., Gilliland, A., Hanna, S., Hogrefe, C., Irwin, J., Rao, S.T., Scheffe, R., Schere, K., Steyn, D., Venkatram, A., 2010. A framework for evaluating regional-scale numerical photochemical modeling systems. *Environ. Fluid Mech.* 10, 471–489.
- Duncan, B.N., Logan, J.A., Bey, I., Megretskaja, I.A., Yantosca, R.M., Novelli, P.C., Jones, N.B., Rinsland, C.P., 2007. Global budget of CO, 1988–1997: source estimates and validation with a global model, 2007. *J. Geophys. Res.* 112, D22301. <http://dx.doi.org/10.1029/2007JD008459>.
- Flemming, J., Inness, A., Flentje, H., Huijnen, V., Moinat, P., Schultz, M.G., Stein, O., 2009. Coupling global chemistry transport models to ECMWF's integrated forecast system. *Geosci. Model Dev.* 2 (2), 253–265. <http://dx.doi.org/10.5194/gmd-2-253-2009>.
- Flemming, J., Huijnen, V., Arteta, J., Bechtold, P., Beljaars, A., Blechschmidt, A.-M., Josse, B., Diamantakis, M., Engelen, R.J., Gaudel, A., Inness, A., Jones, L., Ktragkou, E., Marecal, V., Peuch, V.-H., Richter, A., Schultz, M.G., Stein, O., Tsikerdekis, A., 2014. Tropospheric chemistry in the integrated forecasting system of ECMWF. *Geosci. Model Dev. Discuss.* 7, 7733–7803. <http://dx.doi.org/10.5194/gmd-7-7733-2014>.
- Galmarini, S., Bianconi, R., Appel, W., Solazzo, E., Mosca, S., Grossi, P., Moran, M., Schere, K., Rao, S.T., 2012. ENSEMBLE and AMET: two systems and approaches to a harmonized, simplified and efficient factory for air quality models development and evaluation. *Atmos. Environ.* 53, 51–59.
- Goode, J., Yokelson, R., Ward, D., Susott, R., Babbitt, R., Davies, M., Hao, W., 2000. Measurements of excess O₃, CO₂, CO, CH₄, C₂H₄, C₂H₂, HCN, NO, NH₃, HCOOH, CH₃COOH, HCHO, and CH₃OH in 1997 Alaskan biomass burning plumes by airborne Fourier transform infrared spectroscopy (A-FTIR). *J. Geophys. Res. D Atmos.* 105 (D17), 22147–22166.
- Granier, C., Bessagnet, B., Bond, T., D'Angiola, A., van der Gon, H., Frost, G., Heil, A., Kaiser, J., Kinne, S., Klimont, Z., Kloster, S., Lamarque, J.-F., Liousse, C., Masui, T., Meleux, F., Mieville, A., Ohara, T., Raut, J.-C., Riahi, K., Schultz, M., Smith, S., Thompson, A., van Aardenne, J., van der Werf, G., van Vuuren, D., 2011. Evolution of anthropogenic and biomass burning emissions of air pollutants at global and regional scales during the 1980–2010 period. *Clim. Change* 109 (1), 163–190. <http://dx.doi.org/10.1007/s10584-011-0154-1>.
- Grell, G., Peckham, S., Schmitz, R., McKeen, S., Frost, G., Skamarock, W., Eder, B., 2005. Fully coupled "online" chemistry within the WRF model. *Atmos. Environ.* 39 (37), 6957–6975.
- Hogrefe, C., Hao, W., Zalewsky, E.E., Ku, J.-Y., Lynn, B., Rosenzweig, C., Schultz, M.G., Rast, S., Newchurch, M.J., Wang, L., Kinney, P.L., Sistla, G., 2011. An analysis of long-term regional-scale ozone simulations over the Northeastern United States: variability and trends. *Atmos. Chem. Phys.* 11, 567–582. <http://dx.doi.org/10.5194/acp-11-567-2011>.
- Hogrefe, C., Pouliot, G., Wong, D., Torian, A., Roselle, S., Pleim, J., Mathur, R., 2014. Annual application and evaluation of the online coupled WRF-CMAQ system over North America under AQMEII phase 2. *Atmos. Environ.* 115, 683–694.

- Im, U., Bianconi, R., Solazzo, E., Kioutsioukis, I., Badia, A., Balzarini, A., Baro, R., Bellasio, R., Brunner, D., Chemel, C., Curci, G., Flemming, J., Forkel, R., Giordano, L., Jimenez-Guerrero, P., Hirtl, M., Hodzic, A., Hoznak, L., Jorba, O., Knote, C., Kuenen, J., Makar, P., Manders-Groot, A., Neal, L., Perez, J., Pirovano, G., Pouliot, G., San Jose, R., Savage, N., Schroder, W., Sokhi, R., Syrakov, D., Torian, A., Tuccella, P., Werhahn, J., Wolke, R., Yahya, K., Zabkar, R., Zhang, Y., Zhang, J., Hogrefe, C., Galmarini, S., 2015a. Evaluation of operational online-coupled regional air quality models over Europe and North America in the context of AQMEII phase 2. Part I: ozone. *Atmos. Environ.* 115, 404–420.
- Im, U., Bianconi, R., Solazzo, E., Kioutsioukis, I., Badia, A., Balzarini, A., Baro, R., Bellasio, R., Brunner, D., Chemel, C., Curci, G., van der Gon, H.D., Flemming, J., Forkel, R., Giordano, L., Jimenez-Guerrero, P., Hirtl, M., Hodzic, A., Hoznak, L., Jorba, O., Knote, C., Makar, P., Manders-Groot, A., Neal, L., Perez, J., Pirovano, G., Pouliot, G., San Jose, R., Savage, N., Schroder, W., Sokhi, R., Syrakov, D., Torian, A., Tuccella, P., Wang, K., Werhahn, J., Wolke, R., Yahya, K., Zabkar, R., Zhang, Y., Zhang, J., Hogrefe, C., Galmarini, S., 2015b. Evaluation of operational online-coupled regional air quality models over Europe and North America in the context of AQMEII phase 2. Part II: particulate matter. *Atmos. Environ.* 115, 421–441.
- Inness, A., Baier, F., Benedetti, A., Bouarar, I., Chabrillat, S., Clark, H., Clerbaux, C., Coheur, P., Engelen, R.J., Errera, Q., Flemming, J., George, M., Granier, C., Hadji-Lazarou, J., Huijnen, V., Hurtmans, D., Jones, L., Kaiser, J.W., Kapsomenakis, J., Lefever, K., Leitão, J., Razinger, M., Richter, A., Schultz, M.G., Simmons, A.J., Suttie, M., Stein, O., Thépaut, J.-N., Thouret, V., Vrekoussis, M., Zerefos, C., the MACC team, 2013. The MACC reanalysis: an 8 yr data set of atmospheric composition. *Atmos. Chem. Phys.* 13 (8), 4073–4109. <http://dx.doi.org/10.5194/acp-13-4073-2013>.
- Jaeglé, L., Steinberger, L., Martin, R.L., Chance, K., 2005. Global partitioning of NO_x sources using satellite observations: relative roles of fossil fuel combustion, biomass burning and soil emissions. *Faraday Discuss.* 130, 407–423.
- Johnson, B.T., Osborne, S.R., 2011. Physical and optical properties of mineral dust aerosol measured by aircraft during the GERBILS campaign. *Q. J. R. Meteorol. Soc.* 137 (658), 1117–1130. <http://dx.doi.org/10.1002/qj.777>.
- Kaiser, J.W., Heil, A., Andreae, M.O., Benedetti, A., Chubarova, N., Jones, L., Morcrette, J.-J., Razinger, M., Schultz, M.G., Suttie, M., van der Werf, G.R., 2012. Biomass burning emissions estimated with a global fire assimilation system based on observed fire radiative power. *Biogeosciences* 9, 527–554. <http://dx.doi.org/10.5194/bg-9-527-2012>.
- Katragkou, E., Zanis, P., Tegoulas, I., Melas, D., Kioutsioukis, I., Krüger, B.C., Huszar, P., Halenka, T., Rauscher, S., 2010. Decadal regional air quality simulations over Europe in present climate: near surface ozone sensitivity to external meteorological forcing. *Atmos. Chem. Phys.* 10, 11805–11821. <http://dx.doi.org/10.5194/acp-10-11805-2010>.
- Knote, C., Brunner, D., Vogel, H., Allan, J., Asmi, A., Aijälä, M., Carbone, S., van der Gon, H.D., Jimenez, J.L., Kiendler-Scharr, A., Mohr, C., Poulain, L., Prévôt, A.S.H., Swietlicki, E., Vogel, B., 2011. Towards an online-coupled chemistry-climate model: evaluation of trace gases and aerosols in COSMO-ART. *Geosci. Model Dev.* 4 (4), 1077–1102. <http://dx.doi.org/10.5194/gmd-4-1077-2011>.
- Knote, C., Brunner, D., 2013. An advanced scheme for wet scavenging and liquid-phase chemistry in a regional online-coupled chemistry transport model. *Atmos. Chem. Phys.* 13, 1177–1192. <http://dx.doi.org/10.5194/acp-13-1177-2013>.
- Knote, C., Tuccella, P., Curci, G., Emmons, L., Orlando, J.J., Madronich, S., Baró, R., Jimenez-Guerrero, P., Lueken, D., Hogrefe, C., Forkel, R., Werhahn, J., Hirtl, M., Pérez, J.L., San José, R., Giordano, L., Brunner, D., Yahya, K., Zhang, Y., 2015. Influence of the choice of gas-phase mechanism on predictions of key gaseous pollutants during the AQMEII phase-2 intercomparison. *Atmos. Environ.* 115, 553–568.
- Kuenen, J.J.P., Visschedijk, A.J.H., Jozwicka, M., Denier van der Gon, H.A.C., 2014. TNO MACC II emission inventory: a multi year (2003–2009) consistent high-resolution European emission inventory for air quality modelling. *Atmos. Chem. Phys. Discuss.* 14 (5), 5837–5869. <http://dx.doi.org/10.5194/acpd-14-5837-2014>.
- Lee, C., Martin, R.V., van Donkelaar, A., Lee, H., Dickerson, R.R., Hains, J.C., Krotkov, N., Richter, A., Vinnikov, K., Schwab, J.J., 2011. SO₂ emissions and lifetimes: estimates from inverse modeling using in situ and global, space-based (SCIAMACHY and OMI) observations. *J. Geophys. Res. Atmos.* 116 (D6) <http://dx.doi.org/10.1029/2010JD014758>.
- Makar, P.A., Zhang, J., Gong, W., Stroud, C., Sills, D., Hayden, K.L., Brook, J., Levy, I., Mihele, C., Moran, M.D., Tarasick, D.W., He, H., Plummer, D., 2010. Mass tracking for chemical analysis: the causes of ozone formation in southern Ontario during BAQS-Met 2007. *Atmos. Chem. Phys.* 10, 11151–11173. <http://dx.doi.org/10.5194/acp-10-11151-2010>.
- Miller, S.M., Matross, D.M., Andrews, A.E., Millet, D.B., Longo, M., Gottlieb, E.W., Hirsch, A.I., Gerbig, C., Lin, J.C., Daube, B.C., Hudman, R.C., Dias, P.L.S., Chow, V.Y., Wofsy, S.C., 2008. Sources of carbon monoxide and formaldehyde in North America determined from high-resolution atmospheric data. *Atmos. Chem. Phys.* 8, 7673–7696. <http://dx.doi.org/10.5194/acp-8-7673-2008>.
- Morcrette, J.J., Boucher, O., Jones, L., Salmond, D., Bechtold, P., Beljaars, A., Benedetti, A., Bonet, A., Kaiser, J.W., Razinger, M., Schulz, M., Serrar, S., Simmons, A.J., Sofiev, M., Suttie, M., Tompkins, A.M., Untch, A., 2009. Aerosol analysis and forecast in the European Centre for medium-range weather forecasts integrated forecast system: forward modeling. *J. Geophys. Res. Atmos.* 114, D06206. <http://dx.doi.org/10.1029/2008JD011235>.
- Nédélec, P., Cammas, J.-P., Thouret, V., Athier, G., Cousin, J.-M., Legrand, C., Abonne, C., Lecoœur, F., Cayez, G., Marizy, C., 2003. An improved infrared carbon monoxide analyser for routine measurements aboard commercial airbus aircraft: technical validation and first scientific results of the MOZAIC IIII programme. *Atmos. Chem. Phys.* 3 (5), 1551–1564. <http://dx.doi.org/10.5194/acp-3-1551-2003>.
- Novelli, P., Masarie, K., 2009. Atmospheric Carbon Monoxide Dry Air Mole Fractions from the NOAA ESRL Carbon Cycle Cooperative Global Air Sampling Network, 1988–2008. Tech. rep., NOAA <ftp://ftp.cmdl.noaa.gov/ccg/co/flask/event/>.
- Novelli, P., Masarie, K., 2013. Atmospheric Carbon Monoxide Dry Air Mole Fractions from the NOAA ESRL Carbon Cycle Cooperative Global Air Sampling Network, 1988–2012. version: 2013-06-18. Tech. rep., NOAA ftp://aftp.cmdl.noaa.gov/data/trace_gases/co/flask/surface/.
- Pouliot, G., Denier van der Gon, H., Kuenen, J., Makar, P., Zhang, J., Moran, M., 2015. Analysis of the emission inventories and model-ready emission datasets of Europe and North America for phase 2 of the AQMEII project. *Atmos. Environ.* 115, 345–360.
- Rao, S., Galmarini, S., Keith, P., 2010. Air quality model evaluation international initiative (AQMEII): advancing the state of the science in regional photochemical modeling and its applications. *Bull. Am. Meteorol. Soc.* 92, 23–30.
- Schaub, D., Brunner, D., Boersma, K., Keller, J., Folini, D., Buchmann, B., Berresheim, H., Staehelin, J., 2007. SCIAMACHY tropospheric NO₂ over Switzerland: estimates of NO_x lifetimes and impact of the complex alpine topography on the retrieval. *Atmos. Chem. Phys.* 7 (23), 5971–5987.
- Schere, K., Flemming, J., Vautard, R., Chemel, C., Colette, A., Hogrefe, C., Bessagnet, B., Meuleux, F., Mathur, R., Roselle, S., Hu, R.-Ming, Sokhi, R.S., Rao, S.T., Galmarini, S., 2012. Trace gas/aerosol boundary concentrations and their impacts on continental-scale AQMEII modeling domains. *Atmos. Environ.* 53, 38–50. <http://dx.doi.org/10.1016/j.atmosenv.2011.09.043>.
- Seinfeld, J., Pandis, S., 2006. Atmospheric chemistry and physics: from air pollution to climate change. A Wiley-Interscience publications. Wiley, University of Michigan, USA, p. 1232. ISBN: 0471720186, 9780471720188.
- Sofiev, M., Vankevich, R., Lotjonen, M., Prank, M., Petukhov, V., Ermakova, T., Koskinen, J., Kukkonen, J., 2009. An operational system for the assimilation of the satellite information on wild-land fires for the needs of air quality modeling and forecasting. *Atmos. Chem. Phys.* 9 (18), 6833–6847.
- Solazzo, E., Bianconi, R., Pirovano, G., Moran, M.D., Vautard, R., Hogrefe, C., Appel, K.W., Matthias, V., Grossi, P., Bessagnet, B., Brandt, J., Chemel, C., Christensen, J.H., Forkel, R., Francis, X.V., Hansen, A.B., McKeen, S., Nopmngcol, U., Prank, M., Sartelet, K.N., Segers, A., Silver, J.D., Yarwood, G., Werhahn, J., Zhang, J., Rao, S.T., Galmarini, S., 2013. Evaluating the capability of regional-scale air quality models to capture the vertical distribution of pollutants. *Geosci. Model Dev.* 6 (3), 791–818. <http://dx.doi.org/10.5194/gmd-6-791-2013>.
- Steenefeld, G., Van de Wiel, B., Holtslag, A., 2006. Modeling the evolution of the atmospheric boundary layer coupled to the land surface for three contrasting nights in CASES-99. *J. Atmos. Sci.* 63 (3), 920–935.
- Stein, O., Schultz, M., Flemming, J., Inness, A., Kaiser, J., Jones, L., Benedetti, A., Morcrette, J.-J., 2011. MACC Global Air Quality Services—technical Documentation (Tech. rep., Forschungszentrum Jülich and ECMWF).
- Stein, O., Schultz, M.G., Bouarar, I., Clark, H., Huijnen, V., Gaudel, A., George, M., Clerbaux, C., 2014. On the wintertime low bias of Northern hemisphere carbon monoxide found in global model simulations. *Atmos. Chem. Phys.* 14, 9295–9316. <http://dx.doi.org/10.5194/acp-14-9295-2014>.
- Steinbacher, M., Zellweger, C., Schwarzenbach, B., Bugmann, S., Buchmann, B., Ordez, C., Prevot, A., Hueglin, C., 2007. Nitrogen oxide measurements at rural sites in Switzerland: bias of conventional measurement techniques. *J. Geophys. Res. Atmos.* 112 (11) <http://dx.doi.org/10.1029/2006JD007971>.
- Thouret, V., Marenco, A., Logan, J.A., Nédélec, P., Grouhel, C., 1998. Comparisons of ozone measurements from the MOZAIC airborne program and the ozone sounding network at eight locations. *J. Geophys. Res. Atmos.* 103 (D19), 25695–25720. <http://dx.doi.org/10.1029/98JD02243>.
- Wang, K., Yahya, Y., Zhang, S.-Y.W., Grell, G., 2015. Implementation and initial application of a new chemistry-aerosol option in WRF-Chem for simulation of secondary organic aerosols and aerosol indirect effects for Regional Air Quality. *Atmos. Environ.* 115, 716–732.